Sequence stratigraphic interpretation of peatland evolution in thick coal seams:

Guo, Biao; Shao, Longyi; Hilton, Jason; Wang, Shuai; Zhang, Liang

DOI:
10.1016/j.coal.2018.07.013

Document Version
Peer reviewed version

Citation for published version (Harvard):
Guo, B, Shao, L, Hilton, J, Wang, S & Zhang, L 2018, 'Sequence stratigraphic interpretation of peatland evolution in thick coal seams: Examples from Yimin Formation (Early Cretaceous), Hailaer Basin, China', *International Journal of Coal Geology*, vol. 196, pp. 211-231. https://doi.org/10.1016/j.coal.2018.07.013

Sequence stratigraphic interpretation of peatland evolution in thick coal seams: examples from Yimin Formation (Early Cretaceous), Hailaer Basin, China

Biao Guo [a,b], Longyi Shao [a,*], Jason Hilton [c], Shuai Wang [a], Liang Zhang [a]

[a] *College of Geosciences and Survey Engineering, China University of Mining and Technology, Beijing, 10083, PR China*

[b] *School of Resources and Environment, North China University of Water Resources and Electric Power, Zhengzhou, 450046, Henan, PR China*

[c] *School of Geography, Earth and Environmental Sciences, University of Birmingham, Edgbaston, Birmingham, B15 2TT, UK*

Abstract: Peat formed in mire settings sensitively records environmental fluctuations during deposition including changes in water table or base level and accommodation. On this basis coal seams, as geologically preserved peats, can provide evidence of high-resolution paleoclimatic fluctuations as well as paleobotanical evolution through periods of peat-formation. The No. 2 and No.1 (in ascending order) thick coal seams from the Early Cretaceous Yimin Formation in the Zhalainuoer Coalfield (Hailaer Basin, NE China) are investigated using sedimentological, sequence stratigraphic and petrographic analyses to understand the evolution of their peat forming environments. These 'single' thick coal seams, lacking siliciclasitic partings, are well-developed in the central area of the Zhalainuoer coalfield. Petrographic analyses demonstrate that water-table or base-level fluctuations in 'single' seams can be revealed by a number of significant surfaces formed by various events including paludification, give-up transgressive, accommodation reversal, flooding, and exposure surfaces. These surfaces can separate the single coal into a number of "wetting-up" and "drying-up" cycles. The wetting-up cycle is characterized by a gradual upward increasing trend in the huminite:inertinite ratio and in the ash yields. In contrast, the rapid drying-up cycle is characterized by an upward-increasing trend in the inertinite-dominated coal (46% on average) that represents a phase of exposure and oxidation resulting from a falling water table. This drying-up cycle can be correlated with the scouring surface in landward parts of the basin and terrestrialization surface basinward. The No. 2 coal seam occurs in the transgressive systems tract and comprises three high-frequency depositional sequences in which each coal cycle is characterized by a gradual wetting-up cycle and ends with a rapid drying-up cycle. The No. 1 coal seam occurs in the highstand system tract and consist of several

high-frequency depositional sequences in which each coal cycle is characterized by a gradual drying-up cycle and ends with a rapid wetting-up cycle. These coals could also superpose to constitute the thick coal seam in which various sequence-stratigraphic surfaces can be recognized including terrestrialization, accommodation reversal and exposure surfaces. Stratigraphic relationships between coal and clastic components in the Yimin Formation enable us to demonstrate that thick coals span the formation of several coal cycles and high-resolution boundaries, allowing us to interpret the effects of accommodation on coal seam composition. Recognition that environmental changes can be recorded by thick coals has significance for studies that incorrectly suppose that peat or coal cycles can offer high-resolution and time-invariant records of paleoclimatic fluctuations and paleobotany evolution.

Keywords: Thick coal seam, peat, coal macerals, clastic sediment, petrography, sequence stratigraphy, Hailaer Basin, Cretaceous.

1. Introduction

Peat mires provide a sensitive record of water-table or base-level fluctuations throughout their accumulation (Diessel, 1992, 2007; Jerrett et al., 2010). On this basis, sediments deposited in them can record the long-term evolution of mires and swamps including rates of peat accumulation as well as recording changes in geological environments (Moore, 1989; Kosters and Suter, 1993; Winston, 1994; Banerjee et al., 1996; Bohacs and Suter, 1997; Diessel, 1998; Diessel et al., 2000). Analysis of coal seams using coal petrography, sedimentology, sequence stratigraphy and paleobotany can make comparatively accurate interpretations for conditions of peat formation, not only of the long-term changes of sedimentary environment, but also of short-term sedimentary cycles during peat-forming periods including high-resolution paleoclimatic fluctuation and paleobotanical evolution (Davies et al., 2005, 2006; Jerrett et al., 2010).

For coals to be generated, sufficient accommodation space is required to accumulate peat and to protect it against oxidation or erosion, with accommodation controlled by the height of the water table (Jervey, 1988; Cross, 1988; Bohacs and Suter, 1997). The relationship between accommodation and peat accumulation is thought to be crucial for coal formation (Banerjee et al., 1996; Diessel, 1998; Petersen et al., 1998; Diessel et al., 2000; Holz et al., 2002; Wadsworth et al., 2002, 2003). Coal seams form where the peat accumulation rate balances the accommodation

increasing rate (Bohacs and Suter, 1997; Diessel, 2007), with their long-term balance providing one of the best opportunities to generate thick coal seams.

The "multi-peat superposition genetic model" (Watts, 1971; Shearer et al., 1994; Holdgate et al., 1995; Diessel and Gammidge, 1998; Page et al., 2004; Jerrett et al., 2011) considers that thick coal seams, rather than being the product of single paleo-peat bodies, might represent a succession of stacked mires separated by hiatal surfaces. Generally, autochthonous peat accumulation genesis, of a type mainly occurring in relatively stable tectonic areas, can be subdivided into continuous and discontinuous accumulation of peat, with the difference depending on whether a series of hiatal or non-hiatal surfaces develop during the coal-forming period. By contrast, the "allochthonous accumulation coal-forming model" (Wu, 1994; Wu et al., 1996; Djarar et al., 1997; Wang et al., 1999, 2000, 2001; Wu et al., 2006) has been developed to explain the effects of storms, gravity flow and underwater debris flows discovered in the thick coal seams in small terrestrial fault basins. However, for coal geologists, studies on thick coal seams remain controversial for the following reasons:

(1) It is problematic to reconcile thicknesses of some coal seam with known modern peat thicknesses. Coal seams as much as 100 m thick are often reported in the rock record (e.g. Hu et al., 2011; Wang et al., 2016), whereas the maximum thicknesses for modern peats documented is approximately 20 m (Esterle and Ferm, 1994; Shearer et al., 1994). In view of the appreciable diagenetic compaction of peat after burial, no modern analogue has yet been discovered for the formations of thick coal seams, appearing to challenge the doctrine of ancient analogues for modern conditions. Thus, various researchers have made direct comparison of coal beds with siliciclastic deposits to interpret coal seams as composites of multiple depositional sequences and several significant surfaces (e.g., McCabe, 1984, 1987; Spears, 1987; Greb et al., 2002). Furthermore, these coal seams contain information representing not only the presence of an orderly cycle of peats but also an absence of some hiatal surfaces (Shearer et al., 1994). The recognition of wetting-up and drying-up cycles in coals in response to water-table or accommodation cycles indicates high-frequency paleoclimate changes that may be missed in siliciclastic sediments. Therefore, recognition of vertical and lateral variation of the hiatal surfaces in coal measures, along with separation of an orderly cycle, is of great significance to decipher paleoclimatic fluctuations with the high-resolution and time-significant record in peat successions.

(2) For peat to be preserved, the accommodation rate, mainly controlled by the rate of subsidence and water table level, should approximately balance the rate of peat production (Jervey, 1988; Cross, 1988; Bohacs and Suter, 1997; Wadsworth et al., 2003; Davies et al., 2005). As the accommodation rate goes far beyond peat production, the mire could be drowned with lacustrine, marine or terrestrial sediments, terminating peat accumulation. Likewise, if the accommodation rate falls below the peat production rate, the mire is exposed, becomes oxidized and is replaced by terrigenous clastic sediments. Within the comparatively narrow coal window, the accommodation rate results in the changes to the composition or stacking type of the accumulating peat. Sequence stratigraphy strives to explain sediment superposition and lateral arrangement, which are mainly controlled by the accommodation made below base level relative to the supply rate of sediments (Van Wagoner, 1995; Catuneanu, 2002; Diessel et al., 2007). Therefore, thick coal seams that formed either under a transgressive or regressive regime, contain different single paleo-body stacking patterns and a different composition of the accumulating peat. Recognizing that coals formed in different systems tracts can represent types of cycles of stacked mires has important implications for improving the predictability of vertical and lateral variations in coal composition for mining and coal bed methane projects.

(3) Paragenesis of uranium deposits occasionally accompanies the formation of coal, oil, gas or depositional metallic minerals. In some contexts, coals have even been the important sources of uranium for industrial utilization (Kislyakov and Shchetochkin, 2000; Seredin and Finkelman, 2008; Seredin, 2012). These coals also have high concentrations of other associated elements, including V, Mo, Se, Re and Mn, which may also have potential economic significance (Seredin and Finkelman, 2008; Seredin, 2012; Dai et al., 2015; Finkelman et al., 2018). Coal-hosted U, V and Mo deposits, produced by epigenetic infiltration, have a zoned distribution, which is also a response to the accommodation under a sequence stratigraphic framework (Wu et al., 2009; Guo et al., 2018). Uranium mineralization mainly occurs in coals formed in the highstand or lowstand systems tracts (Yang et al., 2006; Yang et al., 2007; Wu et al., 2009; Guo et al., 2018). The accumulation and mode of occurrence of uranium and rare metals may reflect the original peat-accumulation environments. In other words, coals that selectively preserve some depositional metallic minerals, should relate to where or how the coal was generated and impacted by interaction between peat accumulation and accommodation.

This study is based on the Cretaceous age thick coal seams from the Yimin Formation in the Zhalainuoer coalfield (Hailaer Basin, China), which are widely developed in lacustrine transgression and highstand systems tracts (Zhou et al., 1996; Yuan et al., 2008; Guo et al., 2014). As changes in base level and accommodation are important factors controlling coal accumulation, the succession in the Yimin Formation represents an ideal area to conduct sequence stratigraphic interpretation for mire evolution in thick coal seams. The aims of this paper are to: (1) describe and interpret the thick coal seams and clastic sediments deposited in the Zhalainuoer coalfield, (2) recognize the hiatal or non-hiatal surfaces in the coal seams, (3) interpret the effects of accommodation on coal seam composition and (4) evaluate coal-forming mode in a sequence stratigraphic framework in order to consider how accommodation affects coals deposition.

2. Accommodation and peat/coal formation

During peat accumulation within a mire, the basin subsidence rates and water table control accommodation. The relationship between the change of accommodation rate and peat accumulation rate directly affects peat formation and termination. Bohacs and Suter (1997) studied the phenomenon of modern peat accumulation, and quantified the relationship between the change of the accommodation rate and peat accumulation rate. Peat can accumulate during increasing or decreasing accommodation rates and may span several accommodation cycles (Wadsworth et al., 2002; Jerrett et al., 2010). In cases of high accommodation space, lacustrine or marine fine-grained sediments are firstly developed in the basin, which are not conducive to the formation of peat. As the accommodation space decreases, initiation of peat accumulation above these strata represents a terrestrialization surface (TeS), which is commonly non-hiatal indicating a transition from the shallowing-upward, subaqueous floor deposits to peat accumulation (Diessel et al., 2000; Diessel, 2007; Jerrett et al., 2010; Fig. 1). Only when an equilibrium is reached between the change of accommodation space and peat accumulation rate are optimum conditions met for peat to form with greater thickness. When peat production exceeds the rate of accommodation space, the peat will be exposed, oxidised and eroded. A continued decrease in the accommodation rate finally results in zero accommodation, terminating peat accumulation and generating a subaerial

exposure surface (ExS) or erosional surface (Shearer et al, 1994; Jerrett et al., 2010; Fig. 1); as the accommodation spaces changes from low to high, peat accumulation is gradually established. The initiation of peat accumulation above subaerial, terrigenous strata represents a paludification surface (PaS), which may be hiatal or non-hiatal, depending on the rate of clastic influx (Diessel et al., 2000; Davis et al., 2006; Diessel, 2007; Fig. 1). With a rise in the water table and the accumulation of peat, an equilibrium could also be reached between the accommodation rate and the peat production rate, leading to thicker coal seams being formed. With accommodation gradually increasing, the peat layer is drowned and inundated with fine-grained lacustrine sediments, and the peat formation is terminated at this stage. These two processes were defined as water-regression coal-forming (drying-up cycle) and water-transgression coal-forming (wetting-up cycle) (Bohacs and Suter, 1997; Diessel et al., 2000; Wadsworth et al., 2003; Diessel, 2007; Fig. 1).

In coals, key surfaces or accommodation trends are identified on the basis of petrographic parameters. The water-transgression cycle represents the ratio between the accommodation rate and peat accumulation rate where it is gradually increasing. During the peat forming process, the water table rises causing oxidized fusinite content to reduce and the huminite-inertinite ratio to gradually increase (Diessel, 2007; Jerrett et al., 2010). Moreover, as the water table rises, mineral components in coal seams also increase and the gelification index (GI) gradually rises (Diessel, 2007). This rise in water table contributes to the fact that the coal-forming process is in a reducing environment. The water-regression cycle indicates that the increase rate of the accommodation space is lower than the peat accumulation rate. As the water table falls the GI index gradually decreases, and fusinite and semifusinite content increase (Shearer et al, 1994; Diessel, 2007). This reflects the fact that the coal-forming process is in a weak oxidizing environment with shallow water cover.

3. Geological setting of study area

The Hailaer Basin, with an areal extent of approximately $7.0\times10^{4}km^{2}$, is a Mesozoic-Cenozoic continental basin in northeastern China (Fig. 2A), which developed on the Hercynian fold basement (Zhang, 1992; Cheng, 2006; Wu et al., 2006). The sediment-source

region mainly consists of Sinian-Cambrian metamorphic rocks, Ordovician-Permian marine sedimentary rocks interbedded with epi-metamorphic rocks, and Jurassic volcanic rocks interbedded with volcaniclastics (Chen et al., 2007; Zhang, 2007; Zhang et al., 2015). The Hailaer Basin is flanked by the Great Khingan Mountains to the east, the Northwest Uplift to the west, the Hailatu Mountains and Kuokongduolu Mountains to the north, and the Bayinbolige Uplift to the southeast (Fig.2A). The Basin can be divided into five tectonic units, from west to east comprising the Zhalainuoer Depression, Cuogang Uplift, Beier lake Depression, Bayanshan Uplift and the Huhehu Depression, respectively (Chen et al, 2007; Fig. 2B). These tectonic units also include 16 smaller fault depressions. The coal-bearing strata are part of the Lower Cretaceous Zhalainuoer Group, which consists of the Tongbomiao Formation (K_1t), Nantun Formation (K_1n), Damoguaihe Formation (K_1d) and the Yimin Formation (K_1y) (Wu et al., 2006; Zhang et al., 2015), and mainly comprises conglomerates, medium- to coarse-grained sandstones, siltstones, mudstones and lignites (Zhang et al., 2015). Tectonic evolution in the Hailaer Basin can be subdivided into three stages, namely an initial faulting phase, a faulting-depressing phase and finally a depressing phase (Wu et al., 2006; Zhang et al., 2015). The Yimin Formation was developed in the depressing phase under weaker tectonic activity. Thick coal seams were widely distributed in the mid-upper part of the Yimin Formation where they developed in lacustrine transgression and highstand systems tracts (Li, 1988; Guo, et al., 2014; Zhang et al., 2015; Table 1).

The Zhalainuoer coalfield, with an area of about 480 km^2, is located in the north part of the Zhalainuoer Depression (Fig. 2B). Thick coals mainly occur in the middle of the Yimin Formation, which includes 4-8 seams (Li, 1988; Zhou et al., 1996). The No.2 and No.1 coal seams are the primary economic coal seams in this area and are separated by massive, thick, lacustrine mudstones (Li, 1988; Zhang and Shen, 1991; Zhou et al., 1996; Guo et al., 2015). The Yimin Formation is interpreted as a third-order sequence comprised of several higher frequency fourth-order sequences (Zhou et al., 1996; Yuan et al., 2008; Guo et al., 2014). According to previously conducted sequence stratigraphical analysis, the No. 2 coal seam (including 2-1, 2-2, and 2-3), which ranges from 2-58 m thick, was formed in the lower part of a lacustrine transgressive systems tract which can be subdivided into several fourth-order sequences (Zhou et al., 1996; Guo et al., 2015; Fig. 3). The fourth-order sequence boundaries are characteristic by a stack of erosionally based, conglomeratic and sandstone-dominated distributary channels with

regional extent, which incised the underlying inter-distributary bay siltstones, coal or lacustrine siltstones and mudstones. The depositional environments show the abrupt transitions from lacustrine to delta plain. The lower coal measure (No.2 coal) contains several coal cycles (fourth-order sequences) (Fig. 3), in which the 2-2 and 2-3 coals are the thickest and most laterally extensive coal seams in formation (Li, 1988; Zhou et al., 1996; Guo et al., 2014, 2017). Guo et al. (2014) identified four lithostratigraphic members within the Lower Yimin Formation, each extending shorter distances southward (basinward) than the underlying one as a result of continued retrogradation. This study focusses on the 2-2 and 2-3 coals, which represent two fourth-order sequences, marginal to lacustrine strata, interpreted as discrete packages of fluvial sediments (Zhou et al., 1996; Guo et al., 2014). In the most marginal part of the area, the No. 2 coal is split into two individual seams, separated by a package of fluvial sediments (2-15m thick). Towards the basin, these two coals coalesce and vary from 8-40 m thick. The excellent outcrop exposure in the Zhailainuoer coalfield facilitates sampling and correlation between sections. In the most basinward parts, mudstones interpreted as a set of shallow-lake sediments separate the coal into two seams (Li, 1988; Zhou et al., 1996; Guo et al., 2017). Figure 4 shows a schematic summary of stratigraphic features of the Lower Yimin Formation. The presence of several abrupt vertical discontinuities in the seam is a significant feature of the No. 2 coal. These discontinuities, or abrupt transitions, can be correlated across much of the study area and define what are interpreted as time-equivalent sedimentation units.

The No. 1 coal seam (including 1-1, 1-2, 1-3, and 1-4), which ranges from 1-15 m thick, developed at the top of the Yimin Formation and formed in the middle-late highstand systems tract which can be subdivided into several fourth-order sequences (Zhou et al., 1996; Yuan et al., 2008; Guo et al., 2015; Fig. 3). These high-frequency sequence boundaries are characteristic by the abrupt facies changes, which show the transitions from delta plain or front to lacustrine siltstone and mudstone, reflecting changes in water depth from shallow to deep.

In the Zhalainuoer coalfield coals, vertical root traces can be found in seat earths (Fig. 3), the content of detrital mineral is low (ca. 7.2%, Table 2), coal thickness is relatively stable and evidence of allochthonous peat accumulation genesis such as storms, gravity flow and underwater debris flows have not been identified (Li, 1988; Zhou et al., 2008; Guo et al., 2015). All of these suggest that the No.2 and No.1 coal seams represent mostly autochthonous peat accumulation.

4. Sampling and analytical methods

This study focused on the two thick coals, No. 2 and No.1 in ascending order, of the Zhalainuoer coalfield. Distributions of the sand bodies and coal seams and the important characteristics of the coal facies were analysed to illuminate the differences of mire evolution in the coal-forming processes between the lacustrine transgressive systems tract and highstand systems tract.

A total of 30 samples were taken from the No.2 and No.1 coal seams, including 23 coal bench samples from outcrops of the No. 2 coal and 8 from drill cores for the No.1 coal. All of the coals were sampled with intervals of 1-2 m from top to bottom, and immediately stored in airtight plastic bags and sealed to minimize contamination and oxidation. At the locations where the coal was sampled at outcrop, it was first excavated to a depth of approximately 0.5-1 m in order to remove excessively weathered material. The coal benches are identified by the name of the coalfield (Zhalainuoer with prefix- Z), along with the coal seams numbered in increasing order from top to bottom following Chinese coal geology conventions relating to the order in which they are encountered through drilling. Part of each sample was crushed and ground to 1 mm maximum diameter, bound in epoxy resin as raw coal and then cured, cut and polished on the basis of standard methods for microscopic analysis using white-light reflectance microscopy. Maceral analyses were based on 500 points per sample and the maceral classification and terminology applied in the current study are based on the work of Taylor et al. (1998) and the ICCP System 1994 (ICCP, 1998, 2001). Mean random textinite reflectance was determined from 50 measurements per sample in accordance with Australian Standard guidelines (Australian Standard AS 2856.2-1998. 1998). The remaining parts of samples were crushed and ground to pass through a 200 mesh (75μm) for proximate analysis, conducted on the basis of ASTM Standards D3173-11, D3175-11, and D3174-11 (2011). Total sulfur was determined following ASTM Standard D3177-02 (2002).

5. Results and interpretation

5.1 Coal petrography analysis

5.1.1 Proximate analysis

Table 2 presents proximate analysis results from the No. 2 coal seam collected from outcrop. Ash yield varies greatly through the vertical section from 7.92% to 55.42% (mean = 22.31%), especially in the samples of Z-2-1 and Z-2-2 where ash levels are up to 50%. Total sulfur varies from 0.22% to 1.75% (mean = 0.71%) with high-ash samples also having high sulfur contents. Overall, coals from the Zhalainuoer coalfield are medium-ash and low-sulfur coals.

5.1.2 Maceral analysis

Petrographic analysis shows that coal samples commonly have a high content of huminite, and all of the samples, with the exception of samples Z-2-14, Z-2-15, Z-2-16 and Z-2-17 in the No. 2 coal, have >60% huminite (Fig. 5). The huminite maceral group is dominated by humotelinite (mainly textinite and ulminite, = telohuminite of other authors) (Fig. 6B-E, H) and humodetrinite (Fig. 6G), but is also characterized by gelinite (mainly levigelinite) (Fig. 6A) and corpohuminite (mainly phlobaphinite) (Fig. 6E, F). For huminite to form, it is essential that accumulating plant debris transitions relatively swiftly from the peat surface through oxidizing conditions of the acrotelm into the reducing condition of the catotelm (Diessel et al. 2000). Important to this process is anaerobic bacteria activity that transforms the remaining lignin and cellulose into a partially homogenized humic gel, making huminite. Textinite is indicative of little aerial (aerobic) decay and formed from cell walls (O'Keefe et al., 2013). Textinite is an indicator of a good balance between the rates of accommodation and peat accumulation.

The inertinite maceral group is also common in the samples analyzed, particularly in samples Z-2-14, Z-2-15, Z-2-16 and Z-2-17 where it amounts to >30 vol%. In general, fusinite and semifusinite dominate the inertinite maceral assemblages (Fig. 7A-G, I). Macrinite (Fig. 7H, I) and sclerotinite (Fig. 7J) are also recognized in some of coal samples. Inertinite, particularly fusinite and semifusinite, are the main product of incomplete combustion or oxidation (Guo and Bustin, 1998; Bustin and Guo, 1999; Diessel et al., 2000; Hower et al., 2009, 2011a, b, 2013; O'Keefe and Hower, 2011; O'Keefe et al., 2011, 2013). Thus, high inertinite content, especially structured fusinite and semifusinite (see Fig. 7A-G), can indicate a low or fluctuating mire water-table or comparatively lower accommodation rates relative to peat production (Diessel, 2007; Jerrett et al., 2011).

Liptinite macerals in the coal include sporinite (Fig. 8D), cutinite (Fig. 8C), resinite (Fig. 8A),

and suberinite (Fig. 8B,E). The relatively high huminite to inertinite ratio (e.g. 1:3.97) suggests that the accommodation rate and peat production were well balanced.

The mineral content (Fig. 9A-E) of the coal samples is high with exception of samples Z-2-1 and Z-2-2, with a mean value of 6.0%. Although differing genetically, authigenic minerals are not easy to distinguish from detrital minerals. Nevertheless, as outlined by Moore et al. (1996) in Holocene mires of southeast Asia, authigenic mineral content tends to be quite low unless peat ablation was excessive. Whether generally syngenetic or mostly water-borne in coal samples, minerals are concentrated in coals when the accommodation rate exceeds the rate of peat accumulation. Lower detrital mineral contents mostly occur in coal when the ratio of accommodation nearly balances the rate of peat accumulation. Diessel et al. (2000) suggested that a detrital mineral proportion of less than 10% can be interpreted as oligotrophic peat-forming conditions happening in ombrotrophic raised mires. However, in distal, permanently flooded papyrus marshes around delta plains (McCarthy et al., 1986, 1989; Diessel, 2007), low-ash topogenous peat can form where peat accumulation might be free from the influx of clastic sediment. Detrital mineral contents ranging from 10-30% by volume have been interpreted as eutrophic, limnotelmatic peat-forming conditions where water encroachments were intermittent and frequent so that water-borne minerals can easily migrate in the accumulating peat. Additionally, in some cases, high mineral contents can also occur at the basal coal directly sitting above the seat earth or paleosoil.

5.1.3 TPI and GI

The plant tissue preservation index (TPI) and gelification index (GI), to some extent, can reflect the types of coal-forming plants, sedimentary environments, and other characteristics that affected peat accumulation (Diessel et al., 2000; Davies et al., 2005; Diessel, 2007). On this basis, after the microstructure quantitative analysis of coal seam samples, the TPI and GI of each coal seam sample can be calculated.

Fig. 10 shows the TPI and GI values for the samples studied; all but few TPI values are less than 1, indicating that the coal-forming plants in the coal seam of the study area are mainly dominated by xylophyta with good structural preservation. All of the GI values are >1, reflecting a relatively humid climate. In accordance with the classification basis of the TPI-GI diagram

constructed by Diessel et al. (2000), the coal-forming environments in the study area can be divided into wet forest swamp, forest swamp with shallow overlying water, and lowland swamp. These types of coal facies indicate that the coal-forming swamp environment is mainly a forest peat mire dominated by xylophyta. Also, evolution in the different types of swamp exist in vertical successions through coal seams.

5.2 Interpretation of depositional processes, mire environment and accommodation trends

5.2.1 Thick coal seams in the transgressive systems tract

The No.2 coal seam occurs stratigraphically at the bottom of the Yimin Formation in the Zhalainuoer mining area and developed in the early period of a lacustrine transgressive systems tract. Figure 4 shows a schematic summary of stratigraphic features of the Lower Yimin Formation. The presence of several abrupt vertical discontinuities in the seam is a significant feature of the No. 2 coal. Boreholes zk56-24, zk90-4, zk91-8, as well as outcrop sampling points are selected to analyze the developmental characteristics of the No. 2 Coal seam.

5.2.1.1 Margin of the coalfield

At the most landward locality the No.2 coal is split into two seams vertically (2-2 and 2-3, respectively) by a package of fluvial sediments (Figs. 4, 11). The No. 2-3 coal here sits above a lithofacies association comprising scour-based, poorly sorted, directional conglomerates, cross-bedded sandstones and siltstones or mudstones (Fig. 11). This association is 5-30 m thick in which the predominant trend shows upward-fining cycles and an imbricate arrangement in the basal conglomerates (Fig. 11). These sediments are interpreted as sandy-dominated braided river systems or deltaic distributary channel deposits. Likewise, the No. 2-2 coal also sits above a lithofacies association which consists of scour-based, directional conglomerates, trough cross-bedded sandstones and horizontally bedded mudstones. The differences from the association below No. 2-3 coal are as follows: 1) The basal fine conglomerates or conglomeratic sandstones are thinner and medium- to well-sorted, and clasts have greater sphericity than those below the No. 2-3 coal; 2) The predominant trough cross-bedded sandstones are also medium- to well-sorted and thicker with occasional interbeds of poorly sorted, fine sandstones and carbonaceous mudstones. Coalified plant stems and fragments are common within this facies association. This lithofacies association is interpreted as deltaic distributary channel deposits. Upwards, another sedimentary

364 cycle develops, similar to the fluvial sediments described above, which is finally covered by thick
365 lacustrine mudstones or siltstones with burrows (Figs. 3, 11).
366 Using this information, the coal measures in this area are interpreted to be composed of three
367 high-order sequences (coal-clastic cycles), each typically 10-40 m thick. The sandy-dominated
368 braided river system at the base should been interpreted as having developed in the lowstand
369 systems tract (Figs. 3, 11). The scour-based, poorly sorted, directional conglomerates are
370 interpreted as a sequence boundary. The deeply rooted mudstones underlying the No. 2 coal
371 represents a floodplain deposit. These features are characteristic of a typical river depositional
372 system, in which the gradual nature of the contact between the coal and fine sediments implies
373 that clastic sedimentation was gradually replaced by peat accumulation. The base of the No. 2 coal
374 is therefore interpreted as a non-hiatal paludification surface (PaS1) (Fig. 11). It defines the
375 surface of the initiation of the peat accumulation caused by gradually upward deepening. The
376 gradational nature of the contact between the coal and the overlying carbonaceous mudstone
377 implies that peat accumulation was gradually replaced with lacustrine sediments. This sequence
378 represents a complete wetting-up cycle and the top of the seam is therefore interpreted as a
379 give-up transgressive surface (GUTS) according to Diessel et al. (1999, 2007) (Fig. 11). The
380 second coal-clastic cycle (No. 2-2) is very similar to No. 2-3. The scouring surface is interpreted
381 as the high-resolution sequence boundary where the overlying fluvial sandstones cut down to the
382 top of the No. 2-2 coal (Fig. 11). Within the coal measures in this area, sedimentary trends do not
383 reflect a single period of increasing accommodation. Two coal-clastic cycles may respectively
384 represent a succession of high-resolution, asymmetric cycles, each characterized by a wetting-up
385 cycle that deposited in gradually increasing accommodation (rising water table), and split by
386 scouring surface that represents a sharp decrease in accommodation.
387 5.2.1.2 Centre of the coalfield
388 The coal in center of the coalfield (Fig. 4) sits directly above a fluvial sandstone and is
389 overlain by thick lacustrine mudstones or siltstones with burrows. The coal here is critical to
390 correlating accommodation trends between the landward and the basinward sections because this
391 is a locality where the two coals (No. 2-2 and 2-3) amalgamate and can be sampled conveniently
392 at outcrop. Within the No. 2 coal, petrographic trends reflect several periods of accommodation
393 variation.

394 The seam is divided into three depositional units. In unit 1, the consistently high huminite
395 (70%; table 3) and ash (dry basis) yields (19.8%) indicate that mire conditions may be planar and
396 rheotrophic. The detrital mineral and huminite/inertinite (H/I) trends indicate that peat
397 accumulation occurred during gradually increasing accommodation. On this basis, this unit
398 represents a wetting-up cycle. The low detrital mineral and ash yields of unit 2 demonstrate an
399 almost complete absence of clastic deposits. The high inertinite content, especially the structured
400 subgroups fusinite and semifusinite (Figs. 7, 12.), indicates a lower mire water table and exposure,
401 oxidation or even burning of the peat. Therefore, unit 2 is interpreted as ombrotrophic
402 peat-forming conditions occurring during low accommodation. Unit 3 is subdivided into three
403 smaller wetting-up cycles, which can be interpreted from the vertical petrographic trend. At the
404 top of unit 3, the high of detrital mineral content (up to 20%) represents a planar peat deposited
405 under rheotrophic conditions readily subjected to inundation.
406 Coals in this area consist of three units of coal cycles that are split vertically by petrographic
407 discontinuities. Analysis of mineral and maceral constituents within the three units (Table 3; Fig.
408 12), indicate that they may represent different environments of peat accumulation, including
409 alluvial plains, planar rheotrophic mires, ombrothrophic mires and lacustrine environments. Unit 1
410 and 3 are interpreted as wetting-up cycles, formed in response to gradually increasing
411 accommodation. Unit 2 is interpreted as ombrotrophic peat-forming conditions occurring during
412 lower accommodation, where a low mire water table caused peat exposure, oxidation and
413 combustion.
414 The base of the unit 1 (Fig. 13) is interpreted as a non-hiatal paludification surface (PaS1) in
415 accordance with the interpretation of the margin of the coalfield outlined above. The high
416 inertinite layers developed in unit 2 are analogous to the ‘oxidized organic paring’ of Shearer et al.
417 (1994), who described these as hiatal bounding surfaces between separate, genetic ‘peat bodies’.
418 These are also identical to oxidized layers delineated from the surfaces of Holocene mires, which
419 have ceased peat accumulation due to the increased microbial degradation during periods with
420 depressed water tables (Prokopovich, 1985; Esterle and Ferm, 1994; Cohen and Stack, 1996;
421 Moore et al., 1996; Jerrett et al., 2010). Therefore, this unit implies some degree of hiatus,
422 interpreted as exposure and oxidized organic parting occurring before the initiation of peat
423 accumulation during optimum accommodation. The bounding surface between units 1 and 2

represent an accommodation reversal surface (ARS).

The 3 smaller cycles in unit 3 represent successions of higher-frequency, asymmetrical cycles, each interpreted as a wetting-up cycle that formed during gradually increasing accommodation. These wetting up cycles are separated by surfaces that represent a sharp transition in coal facies interpreted as an abrupt decrease in accommodation. The boundary between the units also represent a surface, of a type amalgamated from a pair of accommodation reversal surface (ARS), while the drying-up constituents of the cycles were temporally transient events such that they are not represented by any thickness of coal. Just as important, these cycles all take on the asymmetric features, which, as demonstrated by Jerrett et al. (2010), can generate as a result of the superposition of high-frequency symmetrical sinusoidal water-table fluctuations in a gradual and steady background trend of water-table rise. This coupled effect would create episodes of abrupt water-table fall when accommodation decreased rapidly.

5.2.1.3 Basinward areas of the coalfield

In the basinward areas of the coalfield, No. 2 coal is split into two seams (2-2 and 2-3) by a package of fine clastic sediments (Figs. 4, 14). The No. 2-3 coal here sits above a lithofacies association which is interpreted as deltaic distributary channel deposits while the No. 2-2 coal sits above a package of fine clastic sediments, which consist of two types of lithofacies associations, namely shore-shallow lacustrine deposits and interfluve paleosols (Fig. 14). The gradational nature of the contact between the No. 2-3 coal and its overlying shore-shallow lacustrine deposits implies that peat accumulation here was gradually replaced by lacustrine sediments. This coal cycle represents a complete wetting-up cycle and the top of the seam is therefore interpreted as a give-up transgressive surface (GUTS) (Fig. 14). The dark grey/brown mudstone with rootlets that commonly underlies the No. 2-2 coal is interpreted as an interfluve paleosol, which can be traced back to a scouring surface at the landward locality (Figs. 4, 14). The top of this paleosol therefore represents a hiatus. The sharp feature of the surface between the coal and the paleosol is in accordance with this interpretation, indicating that the lacustrine sedimentation was not gradually substituted by peat accumulation. The contact surface therefore represents a hiatal paludification surface (PaS2), as it defines the transitional surface from negative accommodation, representing subaerial exposure to positive accommodation (peat accumulation during water-table rise). This surface is equivalent of a scouring surface at the landward locality.

5.2.2 Thick coal seam in the highstand systems tract

The No.1 Coal seam in the Zhalainuoer coalfield developed in the highstand systems tract (HST) period which occurs in the middle of the Yimin Formation. It contains five HST coals, in which the No. 1-1 and 1-2 coals are the thickest and most laterally extensive in the Yimin Formation. Sampling was carried out from borehole cores, where several coal-cycles coalesce. The 8m thick seam rests directly on shallow-lacustrine mudstones (Figs. 3, 15). The base of the coal is therefore interpreted as a terrestrialization surface (TeS) because it represents the initiation of peat accumulation caused by upward shallowing. An ARS occurs 4 m above the base of the seam, which is interpreted as an abrupt deepening event representing a relatively instantaneous transition (Fig. 15). Another ARS overlies this surface and represents a shift to drying-upward cycle. An extensive scouring surface sits directly above the coal, which indicates that the peat was eventually exposed, oxidized and eroded by the fluvial sandstone. All the coal cycles in the HST are interpreted as drying-up cycles, consistent with the interpretation of decreasing accommodation and bounded by ARS representing an abrupt transition in accommodation. The relationship of the No. 1 coal with the underlying and overlying clastic sediments suggests that it generated during a period of gradual decreasing accommodation rate, and represents a transition from lacustrine inundation to subaerial exposure.

6 Discussion

6.1 Stacking types of coal measures in the sequence stratigraphic framework

The type of superposition and lateral distribution of strata are largely controlled by the rate at which accommodation is created below depositional base level, and the rate and mode by which this accommodation is filled with sediments (Vail et al., 1977; Mitchum et al., 1977; Vail, 1987; Van Wagoner et al., 1987, 1990; Jervey, 1988; Shanley and McCabe, 1991). LST sediments are bounded below by a sequence boundary and upward by a first flooding surface. Landward, the intervening deposits are suitable to overlap the sequence boundary. For the low accommodation area, fluvial channels occur extensively, scouring previously deposited alluvial plain sediments.

484 This leads to the development of coarse clastic channel sediments with abundant scour-fill
485 structures, and relatively limited possibilities for peat accumulation (Boyd et al., 1998, Boyd and
486 Leckie, 2000).
487 The Yimin Formation was developed in the basin depressing phase with weaker tectonic
488 activity, and the lake level and climate were the dominant controls on accommodation space, such
489 that the stacking types of strata in the TST in this area are analogous to those in the coastal plain.
490 The TST in this area contains all sediments that are bounded below by the first flooding surface
491 and upward by the maximum flooding surface. The stacking type of deposits is characterized by
492 back-stepping, retrogradational parasequences overlapping the top of the lowstand deposits in the
493 alluvial plain, as a result of the gradually rising base level and increasing accommodation. A large
494 amount of overbank sediment is distributed on the alluvial plain and the transition zone,
495 facilitating the formation and accumulation of peat. Peats also stack in a way consistent with the
496 retrogradational parasequences and extend inland across the alluvial plain (Fig. 16).
497 The HST in this area contains all sediments that are bounded below by the maximum
498 flooding surface and upward by the boundary surface. During the early highstand periods, it
499 provides surplus room for lacustrine deposits under high accommodation settings and thick coal
500 seams can be formed in areas further inland (Boyd and Leckie, 2000). The stacking type of
501 deposits, including coals, are characterized by aggradational parasequences. With the gradual loss
502 of accommodation during the mid- to late highstand periods, rivers migrate more laterally
503 resulting in increasing connectivity of the fluvial sand bodies, pushing the sediments into the basin
504 that form progradational parasequences. This also reduces the possibilities of peat accumulation
505 and causes oxidation and partial or complete erosion of earlier deposits.
506
507 **6.2 Sequence stratigraphic context of the coals**
508
509 Figure 17 shows a generalized accommodation curve and schematic chronostratigraphic chart
510 for the Yimin Formation allowing us to demonstrate the spatial and temporal correlations between
511 the coals and the siliciclastic sediments throughout the study area. The periods of fluvial and
512 lacustrine deposits are based on the stratal geometries shown in Figure 4 and models for sequence
513 formation in the coalfield as described by Guo et al. (2015). The periods of intra-coal seam key

surfaces are based on the interpretations above. This figure shows that where correlatable, accommodation changes are preserved in both coals and siliciclastic sediments.

Within the TST, the strata contains several fourth-order sequences, which are bounded by surfaces that delineate an abrupt transition in petrography representing a rapid decrease in accommodation. This abrupt transition displays diverse spatial and temporal features. The rapid decrease in accommodation can be interpreted as the scouring surfaces (SS) caused by fluvial denudation, the oxidized organic partings in coals characterized by high inertinite and low detrital mineral content, and the paleosol underlying the coals. Therefore, these sequence (or coal cycle) boundaries are represented by scouring surfaces (SS) at the landward locality, but can be traced back the ExS or ARS in coals and the hiatal paludification surfaces (PaS2) at the basinward locality. These bounding surfaces provide time-lines which indicate that the process of paludification was diachronous through the area because the effects from sharp decrease in accommodation or water table on the landward part should have happened sooner than its basinward part. Figure 17 also shows some other points of interest with respect to the amount of time represented by various key sequence-stratigraphic surfaces. The three GUTSs are not synchronous across the study area because they formed throughout the retrogradation of higher-order sequences 1, 2 and 3, respectively. Furthermore, the single GUTS is also slightly diachronous because the basinward part of the termination of peat formation (due to upward deepening) would have been sooner than its landward part because of the topography of the mire.

Within the HST, the strata contains several coal cycles that are bounded by surfaces showing an abrupt transition in petrography representing a rapid increase in accommodation. These higher-order sequence boundaries are represented by scouring surfaces (SS) at the landward locality, but can be traced back the ARS in coals and the hiatal transgressive surface of erosion (TrE) at the basinward locality, which is interpreted as abrupt deepening of facies associated with sediment reworking. The two terrestrialization surfaces (TeS) are also not synchronous across the study area because they formed throughout the protrogradation of coal-cycle 1 and 2, respectively. Furthermore, a single TeS is also slightly diachronous because the landward part of the initiation of peat formation, due to upward shallowing, would have occurred sooner than more basinward part because of the topography of the mire. In addition, Figure 17 shows other intra-coal seam key surfaces which can also correlate spatially and temporally with the siliciclastic components.

6.3 Climate, eustacy and peat formation

Coal preserves a detailed record of the water table fluctuations which can be influenced by the sea-level and/or climatic changes. In paralic coal basins, the water table is mainly controlled by sea level variations which produce systems tracts, sequences and parasequence in siliciclastic sediments or coals (Diessel, 1992). Tornqvist (1993) assumed that relative sea-level changes can impact water tables up to 150 km inland in modern paralic environments. Therefore, water-table fluctuations in the Zhalainuoer coals far from the seas may be mainly controlled by the climate and basin subsidence. In the study area, siliciclastic sediments also reflect the relatively high-frequency climate changes. Drying or wetting events occurring in the siliciclastic sediments can be recognized within the amalgamated coals, and this also provides an opportunity to correlate the siliciclastic sediments with the coal and establish the relative isochronal stratigraphic framework. Compared with siliciclastic sediments, coal, in common with other biochemical sediments, preserves a detailed record of paleoclimate changes so that meaningful information can be obtained from the petrographic analysis of coal down to sample intervals in the centimeter or even millimeter ranges. The recognition of wetting-up and drying-up cycles in coals in response to water-table or accommodation cycles indicates a high-frequency paleoclimate changes which may be missed in the siliciclastic sediments. The three smaller coal-cycles in unit 3 succession, each interpreted as a wetting-up cycle that generated in gradually increasing water-table level, cannot be traced in the adjacent siliciclastic sediments (Figs. 12; 17).

A more complex depositional history can be revealed when the sampling density is increasing and research methods are more comprehensive. Jerrett et al. (2010) recognized six water-table cycles in a Pennsylvanian coal (1.5 m thick) from the Central Appalachia Basin (USA), and assumed that these coal cycles may record Milankovitch to sub-Milankovitch base-level fluctuation periodicities of 0.5 to 17 ka. Lu et al. (2014, 2018) investigated Jurassic coals from the northern Qaidam Basin (China) with a 0.25 m sampling density and indicated that the Milankovitch astronomical cycle is one of the driving forces for coal deposition. In addition, the combination of coal petrography, biomarker and carbon isotope data, and also palynology have become important tools for the reconstruction of paleoclimate and floral changes (Bechtel et al.,

2001, 2007; Otto and Wilde, 2001; Eble et al., 2003; Jasper et al., 2010; Stefanova et al., 2011; Stojanović and Životić, 2013; Gross et al., 2015; Eble and Greb, 2016, 2018). Recognition that the environmental changes can be recorded by the thick coals has significant implication for studies that suppose that peat or coal successions can offer high-resolution and time-significant records of paleoclimatic fluctuations and paleobotany evolution.

7. Conclusions

This survey has demonstrated that coal petrology can provide the possibility to improve sequence stratigraphic interpretations of peatland evolution and thus offer valuable information to the high-resolution record of terrestrial accommodation trends.

Coals can be subdivided into several drying-up or wetting-up cycles. Within the No. 2 coal seams in the transgressive systems tract, five cycles of coal correspond to five high-resolution accommodation periods, in which peat accumulation can be initiated with the advent of paludification surfaces (e.g. non-hiatal PaS1 and hiatal PaS2) and be terminated by flooding surfaces (FS) or giving-up transgressive surfaces (GUTS). These cycles formed during gradually increasing accommodation which is reflected by the increasing concentrations of huminite and detrital minerals associated with a slowed rate of water-table rise. Within the No. 1 coal seam in the highstand systems tract, two drying-up cycles of coal correspond to two high-frequency accommodation cycles, in which peat accumulation can be initiated with terrestrialization surfaces (TeS) and terminated with the flooding surfaces, giving-up transgressive surfaces or transgressive surfaces of erosion (TrE).

Coals have a complex internal sequence stratigraphy which makes it possible to correlate them as terrestrial sediments. The hiatal surfaces (e.g. ARS, PaS2, ExS, TrE) occurring in the coals may be interpreted as the fourth-order sequence boundaries which responded to the sharp drying or wetting events. Within the No. 2 coal seams, some sharp drying-up events terminated the peat accumulation, which can be interpreted as the scouring surfaces (SS) caused by fluvial denudation at the landward locality, the oxidized organic partings (ExS) in coals at the center of the coalfield, and the paleosol underlying the coals (PaS2) at the basinward locality.

Acknowledgements

This research is supported by the National Natural Science Foundation of China (No. 41572090), the Major National Science and Technology Program of China (No. 2016ZX05041004), and High-level Talent Recruitment Project of North China University of Water Resource and Electric (No. 40481). Many thanks are given to Xuetian Wang and Kai Zhou for their help during sample preparation.

References

ASTM Standard D3173-11, 2011. Test Method for Moisture in the Analysis Sample of Coal and Coke. ASTM International, West Conshohochen, PA.

ASTM Standard D3174-11, 2011. Annual Book of ASTM Standards. Test Method for Ash in the Analysis Sample of Coal and Coke. ASTM International, West Conshohochen, PA.

ASTM Standard D3175-11, 2011. Test Method for Volatile Matter in the Analysis Sample of Coal and Coke. ASTM International, West Conshohochen, PA.

ASTM Standard D3177-02, 2002. (Reapproved 2007). Test Methods for Total Sulfur in the Analysis Sample of Coal and Coke. ASTM International, West Conshohochen, PA.

Australian Standard AS 2856.2-1998, 1998. Coal petrography. Part 2: Maceral analysis. Standards Association of Australia, North Sydney, 32 pp.

Banerjee, I., Kalkreuth, W., Davies, E.H., 1996. Coal seam splits and transgressive-regressive coal couplets: a key to stratigraphy of high-frequency sequences. Geology, 24, 1001-1004.

Bechtel, A., Gruber, W., Sachsenhofer, R.F., Gratzer, R., Püttmann, W., 2001. Organic geochemical and stable carbon isotopic investigation of coals formed in low-lying and raised mires within the Eastern Alps (Austria). Organic Geochemistry, 32, 1289-1310.

Bechtel, A., Reischenbacher, D., Sachsenhofer, R.F., Gratzer, R., Lücke, A., Püttmann, W., 2007. Relations of petrographical and geochemical parameters in the middle Miocene Lavanttal lignite (Austria). International Journal of Coal Geology, 134-135, 46-60.

Bohacs, K.M., Suter, J., 1997. Sequence stratigraphic distribution of coaly rocks: fundamental controls and examples. American Association of Petroleum Geologists Bulletin, 81, 1612-1639.

Boyd, R., Diessel, C., Wadsworth, J., Leckie, D., 2000. Organisation of non-marine stratigraphy. In: Boyd, R, Diessel, C.F.K., Francis, S. (Eds.), Advances in the Study of the Sydney Basin. 34th New castle Symposium, Newcastle, NSW, Australia, pp. 1-14.

Boyd, R., Wadsworth, J., Zaitlin, B.A., Dalrymple, R.W., 1998. The stratigraphic organization of incised valley systems. In: Boyd, R., Windwood-Smith, J.A. (Eds.), Advances in the Study of the Sydney Basin. 32nd Newcastle Symposium, Newcastle, NSW, Australia, p. 137.

Bustin, R.M., Guo, Y., 1999. Abrupt changes (jumps) in reflectance values and chemical compositions of artificial charcoals and inertinite in coals. International Journal of Coal Geology, 38, 237-260.

Catuneanu, O., 2002. Sequence stratigraphy of clastic systems: concepts, merits and pitfalls. Journal of African Earth Sciences, 35, 1-43.

Chen, J.L., Wu, H.Y., Zhu, D.F., Lin, C.H., Yu, D.S., 2007. Tectonic evolution of the Hailar Basin and its potentials of oil-gas exploration. Chinese Journal of Geology, 42(1), 147-159. (in Chinese with English abstract).

Cheng, S.Y., 2005. Regional tectonic characters and Meso-Cenozoic basin evolution in northeastern China. Unpublished PhD Thesis, China University of Geosciences (Beijing, China), pp. 1-102. (in Chinese with English abstract).

Cross, A.T., 1988. Controls on coal distribution in transgressive-regressive cycles, Upper Cretaceous, Western Interior, USA. In: Wilgus, C.K., Hastings, B.S., Kendall, C.G.St.C., Posamentier, H.W., Ross, C.A., Van Wagoner, J.C. (Eds.), Sea-Level Changes—An Integrated Approach. Special Publication, vol. 42. Society of Economic Paleontologists and Mineralogists, Tulsa, OK, pp. 371-380.

Cohen, A.D., Stack, E.M., 1996. Some observations regarding the potential effects of doming of tropical peat deposits on the composition of coal beds. International Journal of Coal Geology, 29, 39-65.

Dai, S.F., Yang, J.Y., Ward, C.R., Hower, J.C., Liu, H.D., Garrison, T.M., French, D., O'Keefe, J.M.K., 2015. Geochemical and mineralogical evidence for a coal-hosted uranium deposit in the Yili Basin, Xinjiang, northwestern China. Ore Geology Reviews, 70, 1-30.

Davies, R., Howell, J., Boyd, R., Flint, S., Diessel, C., 2005. Vertical and lateral variation in the petrography of the Upper Cretaceous Sunnyside coal of eastern Utah - implications for the recognition of high-resolution accommodation changes in paralic coal seams. International Journal of Coal Geology, 61, 13-33.

Davies, R., Howell, J., Boyd, R., Flint, S., Diessel, C., 2006. High-resolution sequence-stratigraphic correlation between shallow-marine and terrestrial strata: examples from the Sunnyside Member of the Cretaceous Blackhawk Formation, Book Cliffs, eastern Utah, American Association of Petroleum Geologists Bulletin, 90, 1121-1140.

Diessel, C., 1992. Coal-Bearing Depositional systems. Springer-Verlag, Berlin, Germany.

Diessel, C., 1996. Vitrinite reflectance—more than just a rank indicator? In: Boyd, R.L., Mackenzie, G.A. (Eds.), Advances in the Study of the Sydney Basin. 30th Newcastle Symposium Proceedings, University of Newcastle, Australia, pp. 33-41.

Diessel, C., 1998. Sequence stratigraphy applied to coal seams: two case histories. In: Shanley, K.W., McCabe, P.J. (Eds.), Relative Role of Eustasy, Climate and Tectonism in Continental Rocks. Special Publication, vol. 59. Society of Economic Paleontologists and Mineralogists, Tulsa, OK, pp. 151-173.

Diessel, C., Boyd, R., Wadsworth, J., Leckie, D., Chalmers, G., 2000. On balanced and unbalanced accommodation/peat accumulation ratios in the Cretaceous coals from Gates Formation, Western Canada, and their sequence-stratigraphic significance. International Journal of Coal Geology, 43, 143-186.

Diessel, C., Gammidge, L., 1998. Isometamorphic varations in the reflectance and fluorescence of vitrinite - a key to depositional environment. International Journal of Coal Geology, 36, 167-222.

Diessel, C., 2007. Utility of coal petrology for sequence-stratigraphic analysis. International Journal of Coal Geology, 70, 3-34.

Djarar, L., Wang, H., Guriaud, M., 1997. The Cevennes Stephanian Basin: An example of relationship between sedimentation and late-orogenic extensive tectonics of the Variscan

belt. Geodynamica Acta, 9, 193-222.
Eble, C.F., Pierce, B.S., Grady, W.C., 2003. Palynology, petrography and geochemistry of the Sewickley coal bed (Monongahela Group, Late Pennsylvanian), Northern Appalachian Basin, USA. International Journal of Coal Geology, 55, 187-204.
Eble, C.F., Greb, S.F., 2016. Palynologic, petrographic and geochemical composition of the Vancleve coal bed in its type area, Eastern Kentucky Coal Field, Central Appalachian Basin. International Journal of Coal Geology, 158, 1-12.
Eble, C.F., Greb, S.F., 2018. Geochemical, petrographic and palynologic characteristics of two late middle Pennsylvanian (Asturian) coal-to-shale sequences in the eastern Interior Basin, USA. International Journal of Coal Geology, 190, 99-125.
Esterle, J.S., Ferm, J.C., 1994. Spatial variability in modern tropical peat deposits from Sarawak, Malaysia and Sumatra, Indonesia: analogues for coal. International Journal of Coal Geology, 26, 1-41.
Finkelman, R.B., Palmer, C.A., Wang, P.P., 2018. Quantification of the modes of occurrence of 42 elements in coal. International Journal of Coal Geology, 185, 138-160.
Greb, S.F., Eble, C.F., Hower, J.C., Andrews, W.M., 2002. Multiple-bench architecture and interpretations of original mire phases: examples from the Middle Pennsylvanian of the Central Appalachian Basin, USA. International Journal of Coal Geology, 49, 147-175.
Gross, D., Bechtel, A., Harrington, G.J., 2015. Variability in coal facies as reflected by organic petrological and geochemical data in Cenozoic coal beds offshore Shimokita (Japan)—IODP Exp.337. International Journal of Coal Geology, 152, 63-79.
Guo, B., Shao, L.Y., Ma, S.M., Pei, W.Z., 2015. Lower Cretaceous coal-bearing strata sequence-paleogeography and coal accumulation pattern in Jalai Nur Depression. Coal Geology of China, 27(3), 6-11. (in Chinese with English abstract).
Guo, B., Shao, L.Y., Ma, S.M., Zhang, Q., 2017. Coal-accumulating and coal-forming patterns within sequence stratigraphy framework of Early Cretaceous in Hailar Basin. Coal Geology & Exploration, 45(1), 14-19. (in Chinese with English abstract).
Guo, B., Shao, L.Y., Wen, H.J., Huang, G.N., Zou, M.H., Li, Y.H., 2018. Dual control of depositional facies on uranium mineralization in coal-bearing series: Examples from the Tuanyushan area of the northern Qaidam Basin, NW China. ACTA Geologica Sinica (English edition), 92(2): 733-754.
Guo, B., Shao, L.Y., Zhang, Q., 2014. Sequence stratigraphy and coal accumulation of the Lower Cretaceous coal measures in Hailar Basin. Journal of Palaeogeography, 16(5), 631-640. (in Chinese with English abstract).
Guo, Y., Bustin, R.M., 1998. FTIR spectroscopy and reflectance of modern charcoals and fungal decayed woods: implications for studies of inertinite in coals. International Journal of Coal Geology, 37, 29-53.
Holdgate, G.R., Kershaw, A.P., Slutter, I.R.K., 1995. Sequence stratigraphic analysis and the origins of Tertiary brown coal lithotypes, Latrobe Valley, Gippsland Basin, Australia. International Journal of Coal Geology, 28, 249-275.
Holz, M., Kalkreuth, W., Banerjee, I., 2002. Sequence stratigraphy of paralic coal-bearing strata: an overview. International Journal of Coal Geology, 48, 147-179.
Hower, J.C., Hoffman, G.K., Garrison, T.M., 2013, Macrinite and funginite forms in Cretaceous Menefee Formation anthracite, Cerrillos coalfield, New Mexico. International Journal of

733 Coal Geology, 114, 54-59.
734 Hower, J.C., O'Keefe, J.M.K., Eble, C.F., Raymond, A., Valentim, B., Volk., T.J., Richardson,
735 A.R., Satterwhite, A.B., Hatch, R.S., Stucker, J.D., Watt, M.A., 2011a. Notes on the origin
736 of inertinite macerals in coals: evidence for fungal and arthropod transformations of
737 degraded macerals. International Journal of Coal Geology, 86, 231-240.
738 Hower, J.C., O'Keefe, J.M.K., Volk, T.J., Richardson, A.R., Satterwhite, A.B., Hatch, R.S.,
739 Kostova, I.J., 2011b. Notes on the origin of inertinite macerals in coal: funginite
740 associations with cutinite and suberinite. International Journal of Coal Geology, 85,
741 186-190.
742 Hower, J.C., O'Keefe, J.M.K., Watt, M.A., Pratt, T.J., Eble, C.F., Stucker, J.D., Richardson, A.R.,
743 Kostova., I.J., 2009. Notes on the origin of inertinite macerals in coals: observations on the
744 importance of fungi in the origin of macrinite. International Journal of Coal Geology, 80,
745 135-143.
746 Hu, S.R., Lin, L.N., Huang, C., Chen, D.Y., Hao, G.Q., 2011. Distribution and genetic model of
747 extra-thick coal seams. Coal Geology of China, 3(1), 1-5. (in Chinese with English
748 abstract).
749 International Committee for Coal and Organic Petrology (ICCP), 1998. The new vitrinite
750 classification (ICCP System 1994). Fuel, 77, 349-358.
751 International Committee for Coal and Organic Petrology (ICCP), 2001. The new inertinite
752 classification (ICCP System 1994). Fuel, 80, 459-471.
753 Jasper, K., Hartköpfigkeit-Fröder, C., Flajs, G., Littke, R., 2010. Evolution of Pennsylvanian (Late
754 Carboniferous) peat swamps of the Ruhr Basin, Germany: comparison of palynological,
755 coal petrographical and organic geochemical data. International Journal of Coal Geology,
756 83, 346-365.
757 Jerrett, R. M., Davies, R. C., Hodgson, D. M., Flint, S. S., Chiverrell, R. C., 2011. The
758 significance of hiatal surfaces in coal seams. Journal of the Geological Society, London,
759 168, 629–632.
760 Jerrett, R.M., Flint, S.S., Davies, R.C., Hodgson, D.M., 2010. Sequence stratigraphic
761 interpretation of a Pennsylvanian (Upper Carboniferous) coal from the central Appalachian
762 Basin, USA. Sedimentology, 58(5), 1180-1207.
763 Jervey, M.T., 1988. Quantitative geological modelling of siliciclastic rock sequences and their
764 seismic expression. In: Wilgus, C.K., Hsatings, B.S., Kendall, C.G.St.C., Posamentier,
765 H.W., Ross, C.A., Van Wagoner, J.C. (Eds.), Sea-Level Changes—An Integrated Approach.
766 Special Publication, vol. 42. Society of Economic Paleontologists and Mineralogists, Tulsa,
767 OK, pp. 47-69.
768 Kislyakov, Ya. M., Shchetochkin, V.N., 2000. Hydrogenic ore Formation. Geoinformmark,
769 Moscow (608 pp., in Russian)
770 Kosters, E.C., Suter, J.R., 1993. Facies relationships and systems tracts in the Late Holocene
771 Mississippi Delta plain. Journal of sedimentary Petrology, 59, 98-113.
772 Lu, J., Shao, L.Y., Yang, M.F., Li, Y.H., Zhang, Z.F, Wang, S., Yun, Q.C., 2014. Coal facies
773 evolution, sequence stratigraphy and palaeoenvironment of swamp in terrestrial basin.
774 Jorunal of China Coal Society, 39(12), 2473-2481. (in Chinese with English abstract)
775 Lu, J., Yang, M.F., Sun, X.Y., Shao, L.Y., Zhang, F.H., 2018. Jurassic coal maceral and deposition
776 rate of peat in the northern Qaidam Basin. Journal of Mining Science and Technology, 3(1),

1-8. (in Chinese with English abstract)
Li, S.T., 1988. Fault basin analysis and coal accumulation: an approach to sedimentation, tectonic evolution and energy resource prediction in the Late Mesozoic Fault Basins of northeastern China. Geological Publishing House, Beijing, pp, 1-327.
McCabe, P.J., 1984. Depositional environments of coal and coal-bearing strata. In: Rahmani, R.A., Flores, R.M. (Eds.), Sedimentology of Coal and Coal-Bearing Sequences. Special Publication vol. 7. International Association of Sedimentologists, Oxford, UK, pp. 13-42.
McCabe, P.J., 1987. Facies studies of coal and coal-bearing strata. In: Scott, A.C. (Ed.), Coal and Coal-Bearing Strata: Recent Advances. Special Publication, vol. 32. Geological Society, London, pp. 51-66.
McCarthy, T.S., Ellery, W.N., Roger, K.H., Cairncross, B., Ellery, K., 1986. The roles of sedimentation and plant growth in changing flow patterns in the Okavango Delta, Botswana. South African Journal of Science, 82, 579-584.
McCarthy, T.S., McIver, J.R., Cairncross, B., Ellery, W.N., Ellery, K., 1989. The inorganic chemistry of peat from the Maunchira channel-swamp system, Okavango Delta, Botswana. Geochemica Cosmochimica Acta, 53, 1077-1089.
Mitchum, R.M., Vail, P.R., Thomson, S., 1977. Seismic stratigraphy and changes of sea level. Part 2: the depositional sequence as a basic unit for stratigraphic analysis. In: Payton, C.E. (Ed.), Seismic Stratigraphy-Applications to Hydrocarbon Exploration. Amercian Association of Petroleum Geologists Memoir, vol. 26 pp. 53-62.
Moore, T.A., Shearer, J.C., Miller, S.L., 1996. Fungal origin of oxidized plant material in the Palangkaraya peat deposit, Kalimantan Tengah, Indonesia: implications for ‘inertinite’ formation in coal. International Journal of Coal Geology, 30, 1-23.
Moore, P.D., 1989. The ecology of peat-forming processes—a review. International Journal of Coal Geology, 12, 89-103.
O’Keefe, J.M.K., Bechtel, A., Christanis, K., Dai, S.F., DiMichele, W.A., Eble, C.F., Esterle, J.S., Mastalerz, M., Raymond, A.L., Valentim, B.V., Wagner, N.J., Ward, C.R., Hower, J.C., 2013. On the fundamental difference between coal rank and coal type. International Journal of Coal Geology, 118, 58-87.
O’Keefe, J.M.K., Hower, J.C., 2011. Revisiting Coos Bay, Oregon: a re-examination of funginite-huminite relationships in Eocene subbituminous coals. International Journal of Coal Geology, 85, 65-71.
O’Keefe, J.M.K., Hower, J.C., Finkelman, R.B., Drew, J.W., Stuker, J.D., 2011. Petrographic, geochemical, and mycological aspects of Miocene coals from the Nováky and Handlová mining districts, Slovakia. International Journal of Coal Geology, 87, 268-281.
Otto, A., Wilde, V., 2001. Sesqui-, di-, and triterpenoids as chemosystematic markers in extant conifers — a review. The Botanical Review, 67, 141-238.
Page, S.E., Wüsr, R.A.J., Weiss, D., Rieley, J.Q., Shotyk, W., Limin, S.H., 2004. A record of Late Pleistocene and Holocene carbon accumulation and climate change from an equatorial peat bog (Kalimantan, Indonesia): implications for past, present and future carbon dynamics. Journal of Quaternary Science, 19, 625-635.
Petersen, H.I., Bojesen-Keofoed, J.A., Nytoft, H.P., Surlyk, F., Therkelsen, J., Vosgerau, H., 1998. Relative sea-level changes recorded by paralic liptinite-enriched coal facies cycles, Middle Jurassic Muslingebjerg Formation, Hochstetter Forland, Northeast Greenland. International

Journal of Coal Geology, 36, 1-30.
Prokopovich, N.P., 1985. Subsidence of peat in California and Florida. Bulletin of the Association of Engineering Geologists, 22, 395-420.
Seredin, V.V., 2012. From coal science to metal production and environmental protection: a new story of success. International Journal of Coal Geology, 90-91, 1–3.
Seredin, V.V., Finkelman, R.B., 2008. Metalliferous coals: a review of the main genetic and geochemical types. International Journal of Coal Geology, 76, 253–289.
Shanley, K.W., McCabe, P.J., 1991. Predicting facies architecture through sequence stratigraphy—an example from the Kaiparowits Plateau, Utah. Geology, 19, 742-745.
Shearer, J.C., Staub, J.R., Moore, T.A., 1994. The conundrum of coal bed thickness: a theory for stacked mire sequences. Journal of Geology, 102, 611-617.
Spears, D.A., 1987. Mineral matter in coals, with special reference to the Pennine coalfields. In: Scott, A.C. (Eds.), Coal and Coal-Bearing Strata Recent Advances. Special Publication Geological Society, London, vol. 32., pp. 171-185.
Stefanova, M., Ivanov, D.A., Utescher, T., 2011. Geochemical appraisal of paleovegetation and climate oscillation in the Late Miocene of Western Bulgaria. Organic Geochemistry, 42, 1363-1374.
Stojanović, K., Životić, D., 2013. Comparative study of Serbian Miocene coals—insights from biomarker composition. International Journal of Coal Geology, 107, 3-23.
Taylor, G.H., Teichmüller, M., Davies, A., Diessel, C., Littke, R., Robert, P., 1998. Organic Petrology. Gebrüder Borntraeger, Berlin (704 pp.).
Tornqvist, T.E., 1993. Holocene alternation of meandering and anastomosing fluvial systems in the Rhine-Meuse Delta (central Netherlands) controlled by sea-level rise and subsoil erodibility. Journal of Sedimentary Research, 63, 683-693.
Vail, P.R., 1987. Seismic stratigraphy interpretation procedure. In: Bally, A.W. (Ed.), Atlas of Seismic Stratigraphy. American Association of Petroleum Geologists, vol. 27, pp. 1-10.
Vail, P.R., Mitchum, R.M., Todd, T.G., Widmier, J.M., Thomson III, S., Sangree, J.B., Bubb, J.N., Hatlelid, W.G., 1977. Seismic stratigraphy and global changes of sea level. In: Payton, C.E. (Ed.), Seismic Stratigraphy—Applications to Hydrocarbon Exploration. American Association of Petroleum Geologists. Memoir vol. 26, pp. 49-212.
Van Wagoner, J.C., 1995. Sequence stratigraphy and marine to nonmarine facies architecture of foreland basin strata, Book Cliffs, Utah, USA. In: Van Wagoner, J.C., Bertram, G.T. (Eds.), Sequence Stratigraphy of Foreland Basin Deposits, Outcrop and Subsurface Examples from the Cretaceous of North America. Memoir vol. 64. American Association of Petroleum Geologists, Tulsa, OK, pp. 137-223.
Van Wagoner, J.C., Mitchum, R.M., Campion, K.M., Rahmanian, V.D., 1990. Siliciclastic sequence stratigraphy in well logs, cores and outcrop: concepts for high resolution correlation of time and facies. Amercian Assocication of Petroleum Geologists, Methods Exploration, Ser. 7, 64.
Van Wagoner, J.C., Mitchum, R.M., Posamentier, H.W., Vail, P.R., 1987. The key definitions of sequence stratigraphy. In: Bally, A.W. (Ed.), Atlas of Sequence Stratigraphy. American Association of Petroleum Geologists Studies in Geology, vol. 1, pp. 27.
Wadsworth, J., Boyd, R., Diessel, C., Leckie, D., 2003. Stratigraphic style of coal and non-marine strata in a high accommodation setting: Fahler Member and Gates Formation (Lower

Cretaceous), western Canada. Bulletin of Canadian Petroleum Geology, 51, 275-303.
Wadsworth, J., Boyd, R., Diessel, C., Leckie, D., Zaitlin, B.A., 2002. Stratigraphic style of coal and non-marine strata in a tectonically influenced intermediate accommodation setting: the Mannville Group of the Western Canadian Sedimentary Basin, south-central Alberta. Bulletin of Canadian Petroleum Geology, 50, 507-541.
Wang, D.D., Shao, L.Y., Liu, H.Y., Shao, K., Yu, D.M., Liu, B.Q., 2016. Research progress in formation mechanisms of super-thick coal seam. Journal of China Coal Society, 41(6), 1487-1497. (in Chinese with English abstract).
Wang, H., Wu, C.L., Courel, L., Guiraud, M., 1999. Analysis on accumulation mechanism and sedimentary conditions of thick coalbeds in Sino-French faulted coal basins, Earth Science Frontier (China University of Geosciences), 6(S1), 157-166. (in Chinese with English abstract).
Wang, H., Xiao, J., Zhang, R.S., Wang, G.F., Yang, H., 2000. Review of analysis on the sedimentary conditions of thick coalbeds. Geological Science and Technology Information, 19(3), 44-49. (in Chinese with English abstract).
Wang, H., Zheng, Y.T., Yang, H., 2001. Analysis on the sedimentary conditions of thick coalbeds in French faulted coal basin. Coal Geology & Exploration, 29(1), 1-4. (in Chinese with English abstract).
Watts, W.A., 1971. Postglacial and interglacial vegetation history of southern Georgia and central Florida. Ecology, 52, 676-690.
Winston, P.B., 1994. Models of the geomorphology, hydrology and development of domed peat bodies. Geological Society of America Bulletin, 106, 1594-1604.
Wu, C.L., 1994. The genesis model of the coal and extra-thick coal seam in the Fushun Basin. Chinese Science Bulletin, 39(23), 2175-2177. (in Chinese with English abstract).
Wu, C.L., Li, S.H., Huang, F.M., Zhang, R.S., Wang, H.Q., Zhao, L.G., 1996. Analysis on sedimentary conditions of extra-thick coal seam from Fushun coalfield. Coal Geology and Exploration, 25(2), 1-6. (in Chinese with English abstract).
Wu, C.L., Li, S.H., Wang, G.F., Liu, G., Kong, C.F., 2006. Genetic model about the extra-thick and high quality coalbed in Xianfeng Basin, Yunnan Province, China. Acta Sedimentologica Sinica, 24(1), 1-9. (in Chinese with English abstract).
Wu, G.Y., Feng, Z.Q., Yang, J.G., Wang, Z.J., Zhang, L.G., Guo, Q.X., 2006. Tectonic setting and geological evolution of Mohe basin in northeast China. Oil and Gas Geology, 27(4), 528-535. (in Chinese with English abstract).
Wu, L.Q., Jiao, Y.Q., Roger, M., Yang, S.K., 2009. Sedimentological setting of sandstone-type uranium deposits in coal measures on the southwest margin of the Turpan-Hami Basin, China. Journal of Asian Earth Sciences, 36(2): 223–237.
Yang, M.H., Liu, C.Y., 2006. Sequence stratigraphic framework and its control on accumulation of various energy resources in the Mesozoic continental basins in Ordos. Oil and Gas Geology, 27(4), 563–570. (in Chinese with English abstract).
Yang, R.C., Han, Z.Z., Fan, A.P., 2007. Sedimentary microfacies and sequence stratigraphy of sandstone-type uranium deposit in the Dongsheng area of the Ordos Basin. Journal of Stratigraphy, 31(3), 261–266 (in Chinese with English abstract).
Yuan, H.Q., Liu, C.Z., Zhao, L.H., Zhang, W.H., Lü, Y.F., 2008. Study on the Lower Cretaceous sequence stratigraphy and depositional systems in the Chagannuoer Depression of the

Hailaer Basin. Journal of Stratigraphy, 32(4), 397-408. (in Chinese with English abstract).
Zhang, F., 2007. The structural feature and tectonic evolution about Hai Laer Basin. Jilin University (Ph. D thesis), pp. 1-99. (in Chinese with English abstract)
Zhang, J.G., 1992. Similarity and diversity between Hailar Basin and Erlian Basin. Petroleum Exploration & Development, 19(6), 15-22. (in Chinese with English abstract).
Zhang, J.L., Shen, F., 1991. Sedimentary properties of Zhalainuoer Group in Hailar Basin. Oil and Gas Geology, 12(4), 417-425. (in Chinese with English abstract).
Zhang, X.Z., Guo, Y., Zeng, Z., Fu, Q.L., Pu, J.B., 2015. Dynamic evolution of the Mesozoic-Cenozoic basins in the northeastern China. Earth Science Frontiers, 22(3), 88-98. (in Chinese with English abstract).
Zhou, J.Y., Liu, C.Q., Li, J.F., 1996. Fill-sequences and coal-accumulating rules of sedimentary basin in Hailar area. Coal Geology and Exploration, 24(2), 1-5. (in Chinese with English abstract).

Figure captions

Fig 1. (A) Idealized curve showing the relationship between accommodation and peat production, and the coal window of Bohacs and Suter (1997) with the genetic pathways of two seams, A and B (modified after Wadsworth et al., 2003 and Diessel, 2007). (B) Sequence stratigraphic interpretation of drying-up or wetting-up cycle, and stratigraphic sections through coal beds showing the vertical and lateral variation of the significant surfaces. SB = sequence boundary, MFS = maximum flooding surface, BSFR = basal surface of forced regression, MRS = maximum regression surface, HNR = highstand normal regression, FR = forced regression, LNR = lowstand normal regression, LST = lowstand systems tract, TST = transgressive systems tract, HST = highstand systems tract.

Fig. 2. (A) Location of the Hailaer Basin in China. (B) Geotectonic divisions of the Hailaer Basin and location of the Zhalainuoer coalfield (modified from Wu et al., 2006). (C) Geological sketch map of the Zhalainuoer coalfield. (D) A cross-section of the Zhailainuoer coalfield (location of section in (C), modified from Guo et al., 2014). J_2tm, Middle Jurassic Tamulangou Formation; J_3mk, Upper Jurassic Manketouebo Formation; J_3mn, Upper Jurassic Manitu Formation; J_3b, Baiyingaolao Formation. K_1t, Lower Cretaceous Tongbomiao Formation; K_1n, Lower Cretaceous Nantun Formation; K_1d, Lower Cretaceous Damoguaihe Formation; K_1y, Lower Cretaceous Yimin Formation; Q, Quaternary.

Fig. 3. Relationship between stratigraphic fabric and coal accumulation in the Yimin Formation. SB= sequence boundary, MFS= maximum flooding surface, FFS= first flooding surface, SL= shallow lake, LS= shore lake, DF= delta front, DP= delta plain.

Fig. 4. Schematic cross section showing vertical and lateral variation of the No. 2 coal seam in the Zhalainuoer coalfield. A-B refers to the section line in the locality map (Fig. 2). Grey in the right-down figure represents coals.

Fig. 5. Bar chart of maceral content of the studied coal samples.

Fig. 6. Huminite in the Zhalainuoer coals under reflected white light microscopy. (A), Levigelinite. (B), Ulminite (left) adjacent to semifusinite (right), and sporopolleninite. (C), Textinite. (D), Ulminite. (E), Phlobaphinite. (F), Ulminite (left) adjacent to corpohuminite (right). (G), Ulminite and attrinite. (H), Textinite.

Fig. 7. Inertinite in coal under reflected white light microscopy. (A), Fusinite. (B), Semifusinite with ‘bogen’ structure. (C), Pyrofusinite. (D), Fusinite with cell structure. (E), Broken semifusinite. (F), Thickened cell walls in semifusinite. (G), Pyrofusinite and macrinite. (H), Macrinite. (I), Rounded oxymacrinite (degraded macrinite), macrinite and semifusinite. (J), Sclerotinite.

Fig. 8. Liptinite maceral group in the Zhalainuoer coals under the reflected white light microscopy. (A), Cells (fusinite) infilled with resinite. (B), Suberinite with phlobaphinite. (C), Cutinite. (D), Sporopolleninite. (E), Suberinite with imbricate arrangement.

Fig. 9. Mineral in the Zhalainuoer coals under the reflected white light microscopy. (A) and (B), Calcite. (C) and (D), Pyrite. (E), Clay

Fig. 10. Coal facies deciphered from tissue preservation index (TPI) and gelification index (GI) in relation to depositional setting and type of mire (Diessel et al. 2000)

Fig. 11. Generalized accommodation curve and mire evolution for the duration of the deposition in the margin of the coalfield, based on trends identified in the boreholes.

Fig. 12. Schematic cross section showing the vertical and lateral variation of the No. 2 coal seam in the Zhalainuoer coalfield.

Fig. 13. Generalized accommodation curve and mire evolution for the duration of the deposition at the center of the Zhalainuoer coalfield, based on trends identified in the boreholes.

Fig. 14. Generalized accommodation curve and mire evolution for the duration of the deposition at the basinward locality of the Zhalainuoer coalfield, based on trends identified in the boreholes.

Fig. 15. Generalized accommodation curve and mire evolution for the duration of the deposition of highstand system tracts, based on trends identified in the boreholes.

Fig. 16. Superposition and lateral distribution of strata in Zhalainuoer coalfield.

Fig. 17. Schematic chronostratigraphic chart showing the spatial and temporal correlation of the Zhailainuoer coals with interpreted sequence stratigraphic surfaces.

Table Captions

Table 1. Sequence-stratigraphic position of various coalfields within the framework of systems tracts in Hailaer Basin (Guo, et al., 2014). ▲= coal, DM = Dongming, ZLNR = Zhalainur, HHH = Huhehu, YM = Yimin, HQ = Hongqi, WRX = Wuerxun, HEHD = Heerhongde, MDMJ = Modamuji, JQ = Jiuqiao, BR = Beier, MDH = Mianduhe.

Table 2. Proximate analysis of the coals from studied area. M, moisture; A, ash yield; St, total sulfur; ad, as-received basis; d, dry basis; daf, dry and ash-free basis.

Table 3. Petrographic composition determined under optical microscope for coals from Hailaer Basin (vol %). T-I, total inertinite. T-H, total huminite. F, fusinite. HT, humotelinite. HD, humodetrinite. HC, humocollinite. ID, inertodetrinite. H/I, huminite -to-inertinite ratio. Min, mineral.

1010 Figure 1

1011

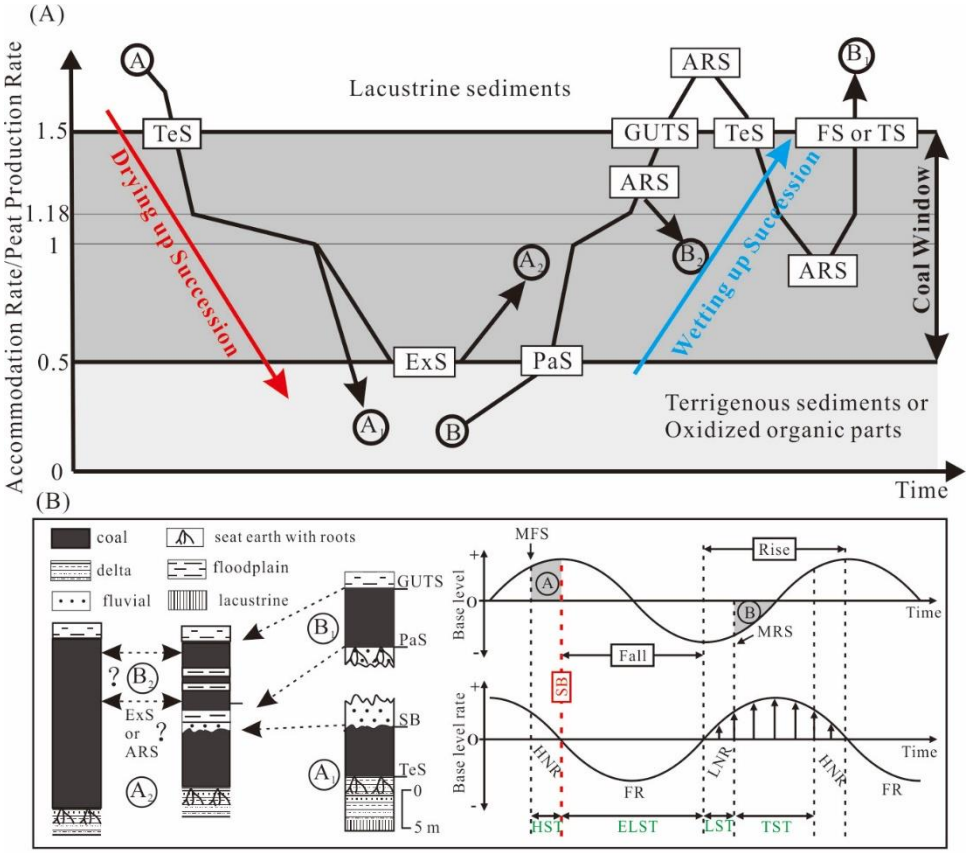

	Surface	Explanation	Attribute of origin
TeS	Terrestrialization Surface	Initiation of peat formation caused by upward shallowing	Nohiatal
PaS	Paludification Surface	Initiation of peat formation caused by upward deepening	Nohiatal or Hiatal
GUTS	Give-up Transgressive Surface	Gradual termination of peat formation caused by upward deepening	Nohiatal
ARS	Accommodation Reversal Surface	Transition between shallowing and deepening upward(and vice versa)	Nohiatal or Hiatal
FS	Flooding Surface	Abrupt deepening of sediments	Hiatal
ExS	Exposure Surface	Exposure or Oxidation organic parting	Hiatal

1012

1013

Figure 2

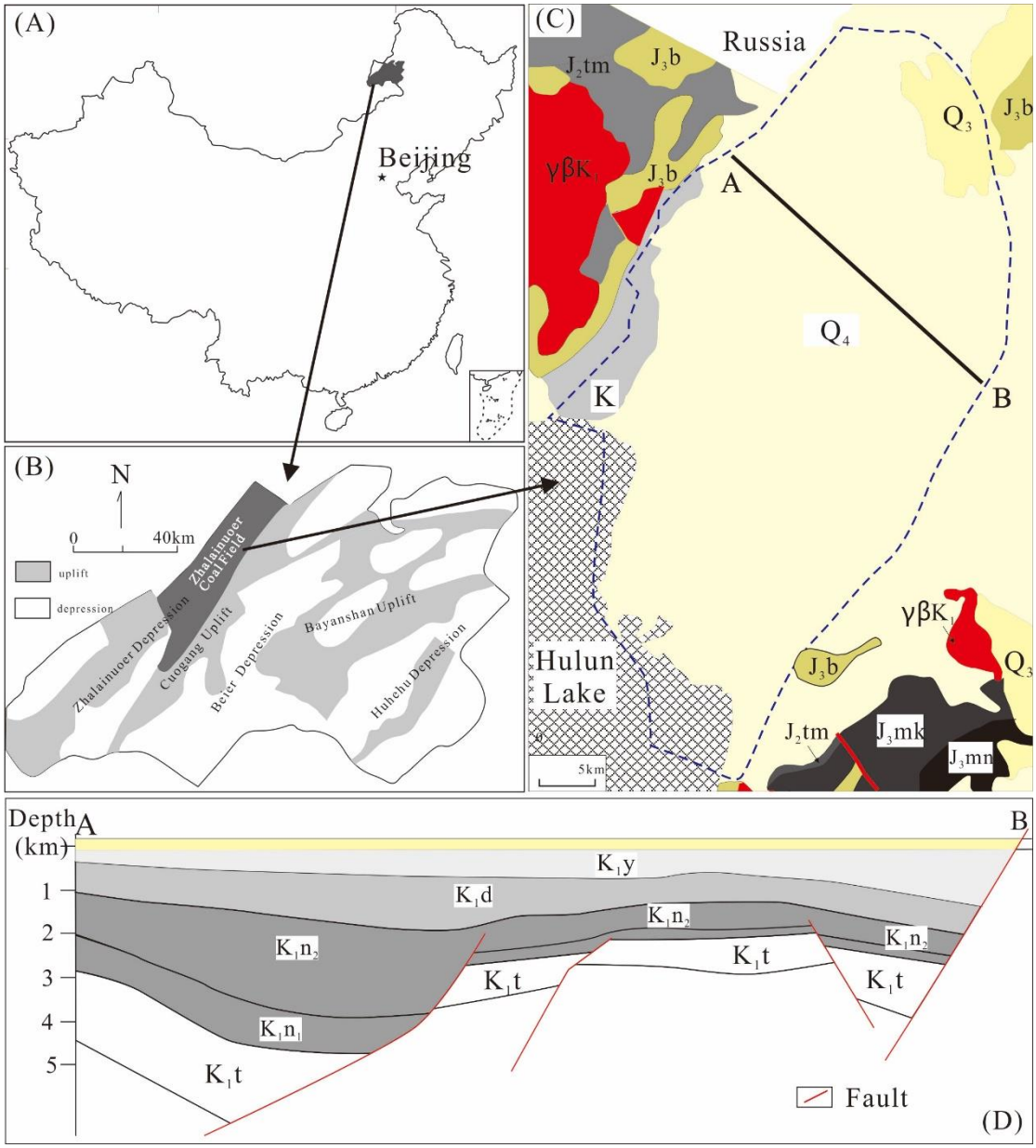
(A)
Beijing
(B)
N
0
40km
uplift
depression
Zhalainuoer Coal Field
Zhalainuoer Depression
Cuogang Uplift
Beier Depression
Bayanshan Uplift
Huhehu Depression
(C)
Russia
J_2tm
J_3b
$\gamma\beta K_1$
Q_3
A
B
Q_4
K
Hulun Lake
5km
(D)
Depth (km)
A
B
K_1y
K_1d
K_1n_2
K_1n_1
K_1t
Fault

Figure 3

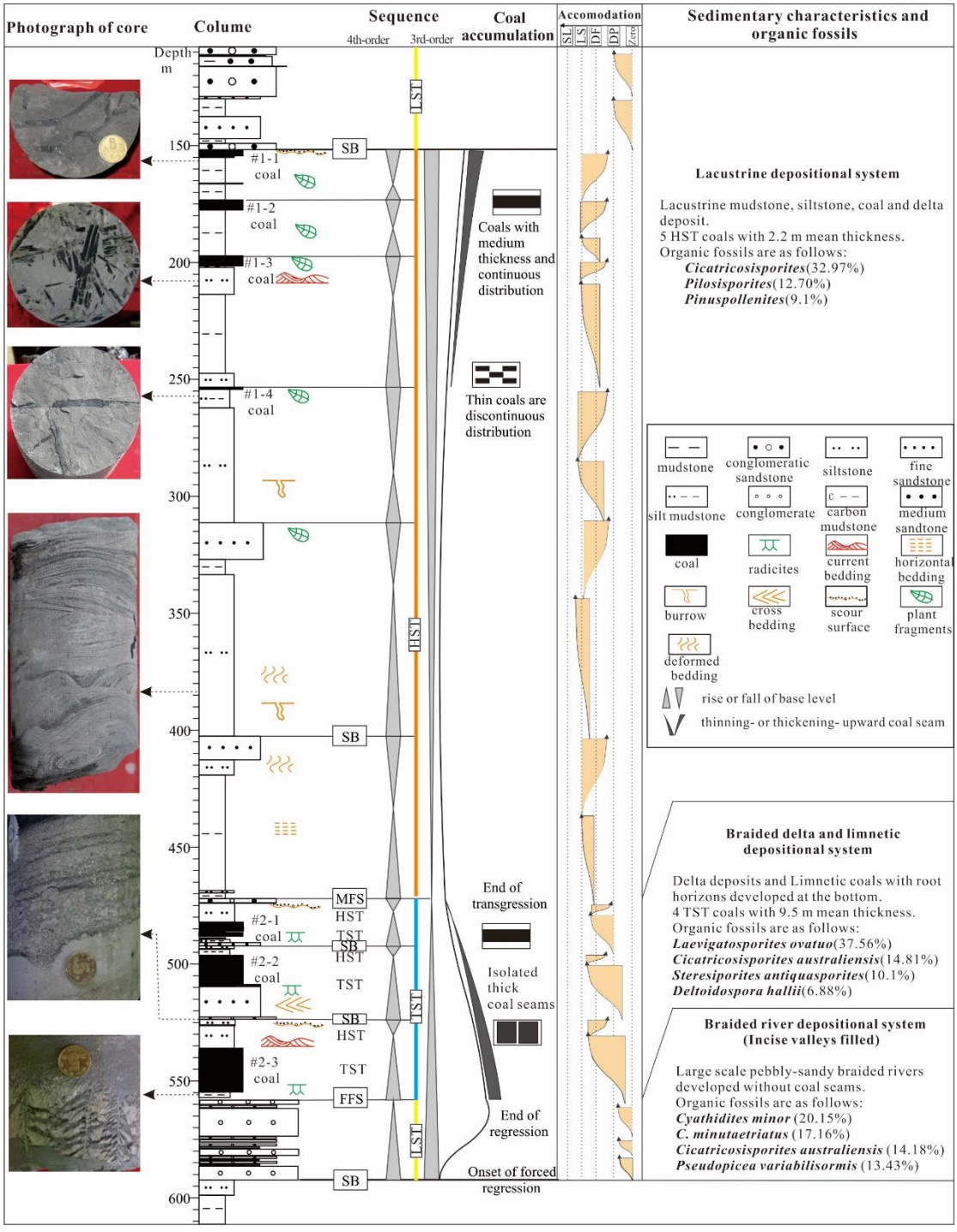
Photograph of core
Colume
Sequence
4th-order
3rd-order
Coal accumulation
Accomodation
SL
LS
DF
DP
Zero
Sedimentary characteristics and organic fossils
Depth m
150
200
250
300
350
400
450
500
550
600
#1-1 coal
#1-2 coal
#1-3 coal
#1-4 coal
#2-1 coal
#2-2 coal
#2-3 coal
SB
MFS
FFS
HST
TST
LST
Coals with medium thickness and continuous distribution
Thin coals are discontinuous distribution
End of transgression
Isolated thick coal seams
End of regression
Onset of forced regression
Lacustrine depositional system
Lacustrine mudstone, siltstone, coal and delta deposit.
5 HST coals with 2.2 m mean thickness.
Organic fossils are as follows:
Cicatricosisporites(32.97%)
Pilosisporites(12.70%)
Pinuspollenites(9.1%)
mudstone
conglomeratic sandstone
siltstone
fine sandstone
silt mudstone
conglomerate
carbon mudstone
medium sandtone
coal
radicites
current bedding
horizontal bedding
burrow
cross bedding
scour surface
plant fragments
deformed bedding
rise or fall of base level
thinning- or thickening- upward coal seam
Braided delta and limnetic depositional system
Delta deposits and Limnetic coals with root horizons developed at the bottom.
4 TST coals with 9.5 m mean thickness.
Organic fossils are as follows:
Laevigatosporites ovatuo(37.56%)
Cicatricosisporites australiensis(14.81%)
Steresiporites antiquasporites(10.1%)
Deltoidospora hallii(6.88%)
Braided river depositional system (Incise valleys filled)
Large scale pebbly-sandy braided rivers developed without coal seams.
Organic fossils are as follows:
Cyathidites minor (20.15%)
C. minutaetriatus (17.16%)
Cicatricosisporites australiensis (14.18%)
Pseudopicea variabilisormis (13.43%)

Figure 4

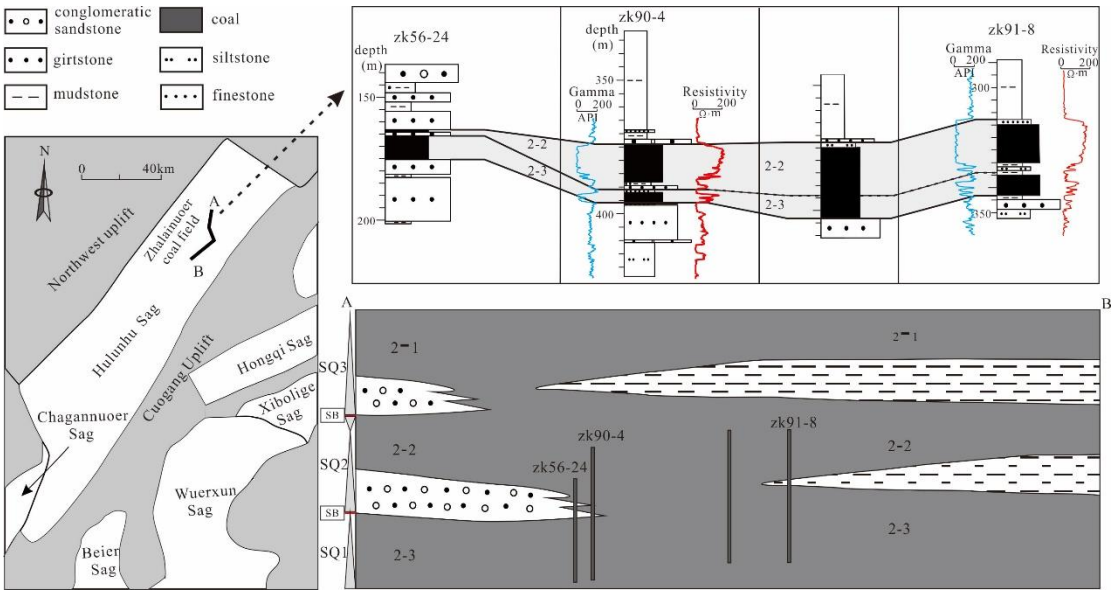
conglomeratic sandstone
coal
girtstone
siltstone
mudstone
finestone
N
0
40km
Northwest uplift
Zhalainuoer coal field
A
B
Hulunhu Sag
Cuogang Uplift
Honggi Sag
Xibolige Sag
Chagannuoer Sag
Wuerxun Sag
Beier Sag
zk56-24
zk90-4
zk91-8
depth (m)
Gamma API
Resistivity Ω·m
2-2
2-3
SQ3
SQ2
SQ1
SB

1026 Figure 5

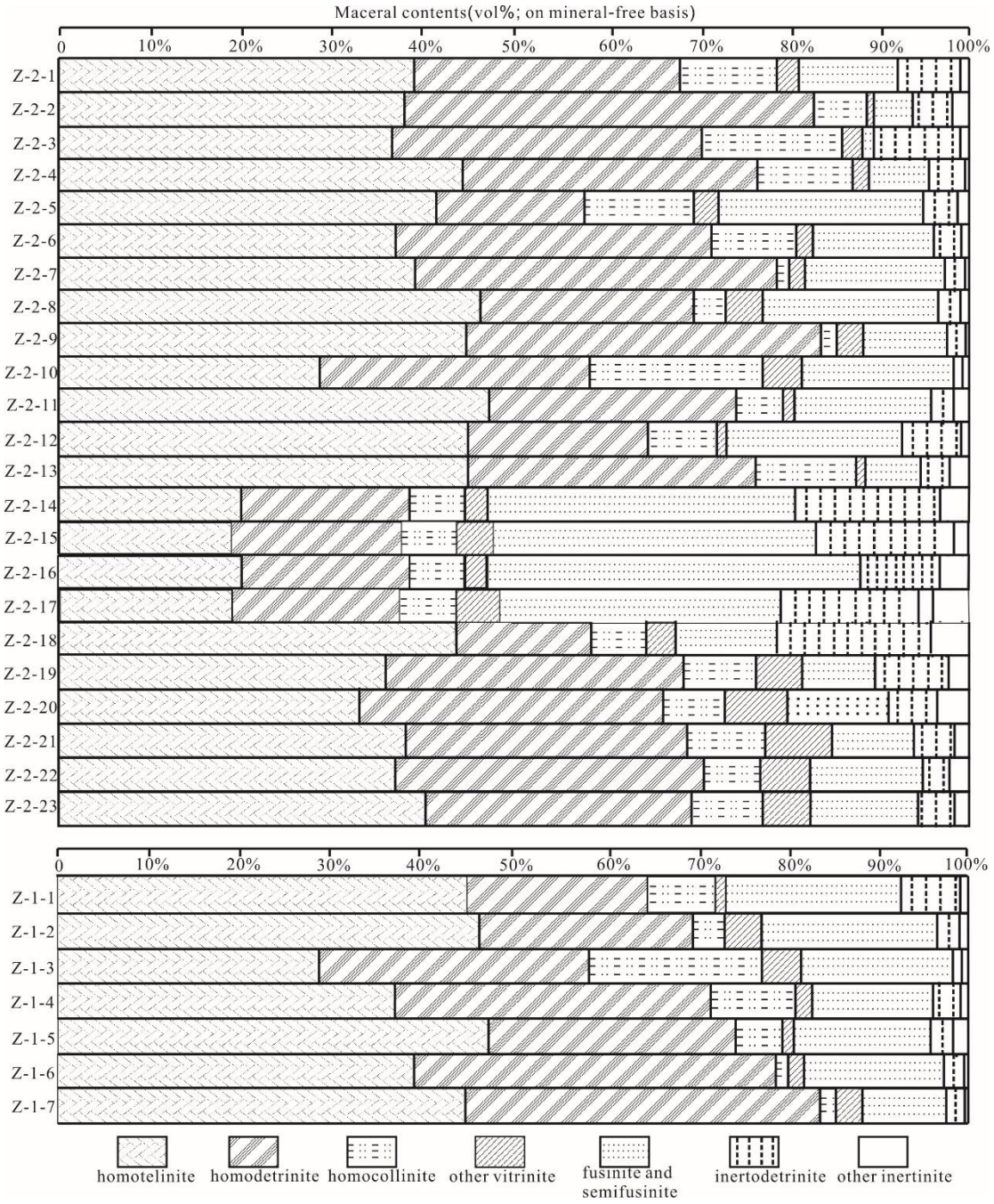

1027

1028

Figure 6

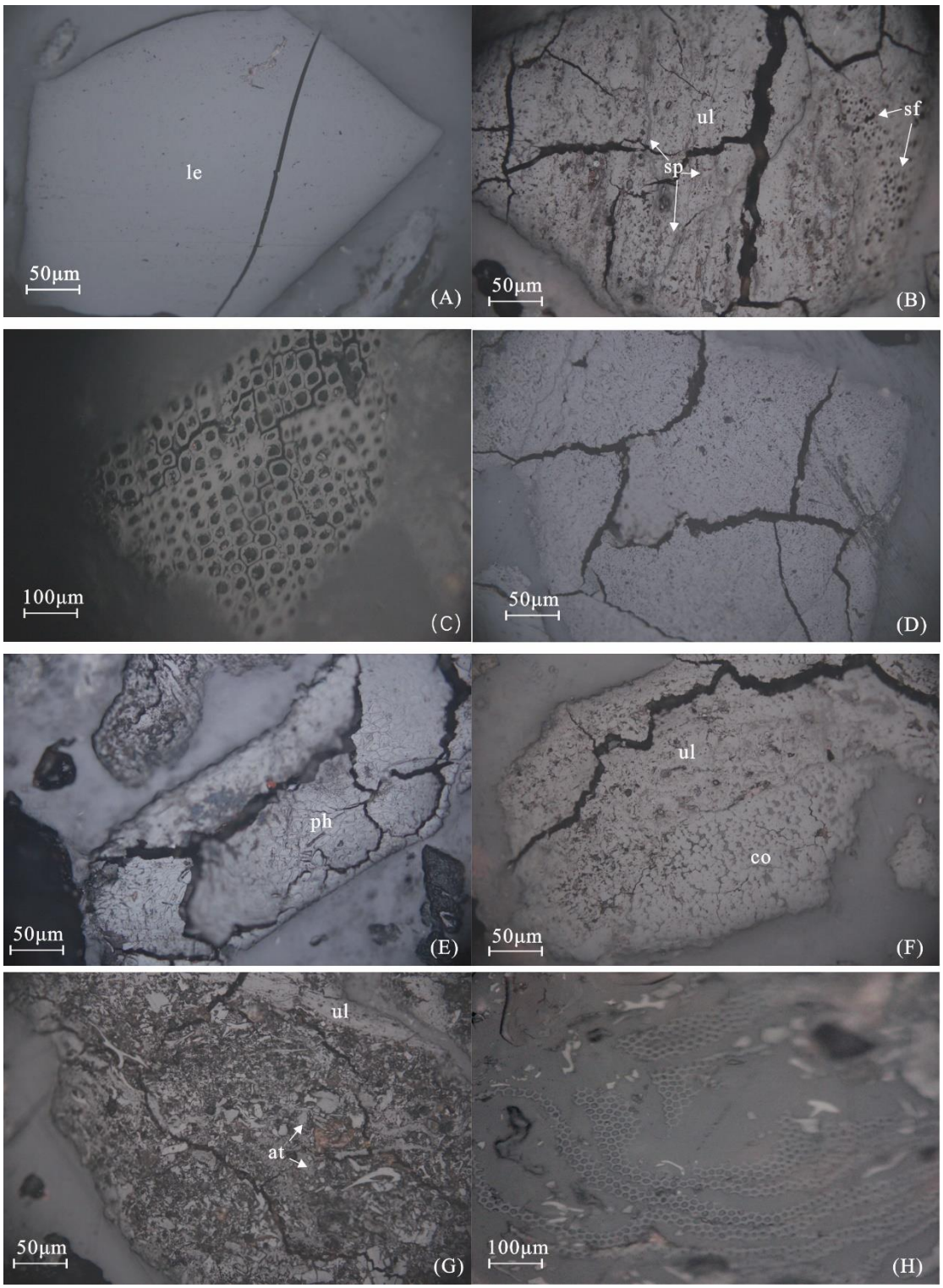
le
50μm
(A)
ul
sp
sf
50μm
(B)
100μm
(C)
50μm
(D)
ph
50μm
(E)
ul
co
50μm
(F)
ul
at
50μm
(G)
100μm
(H)

Figure 7

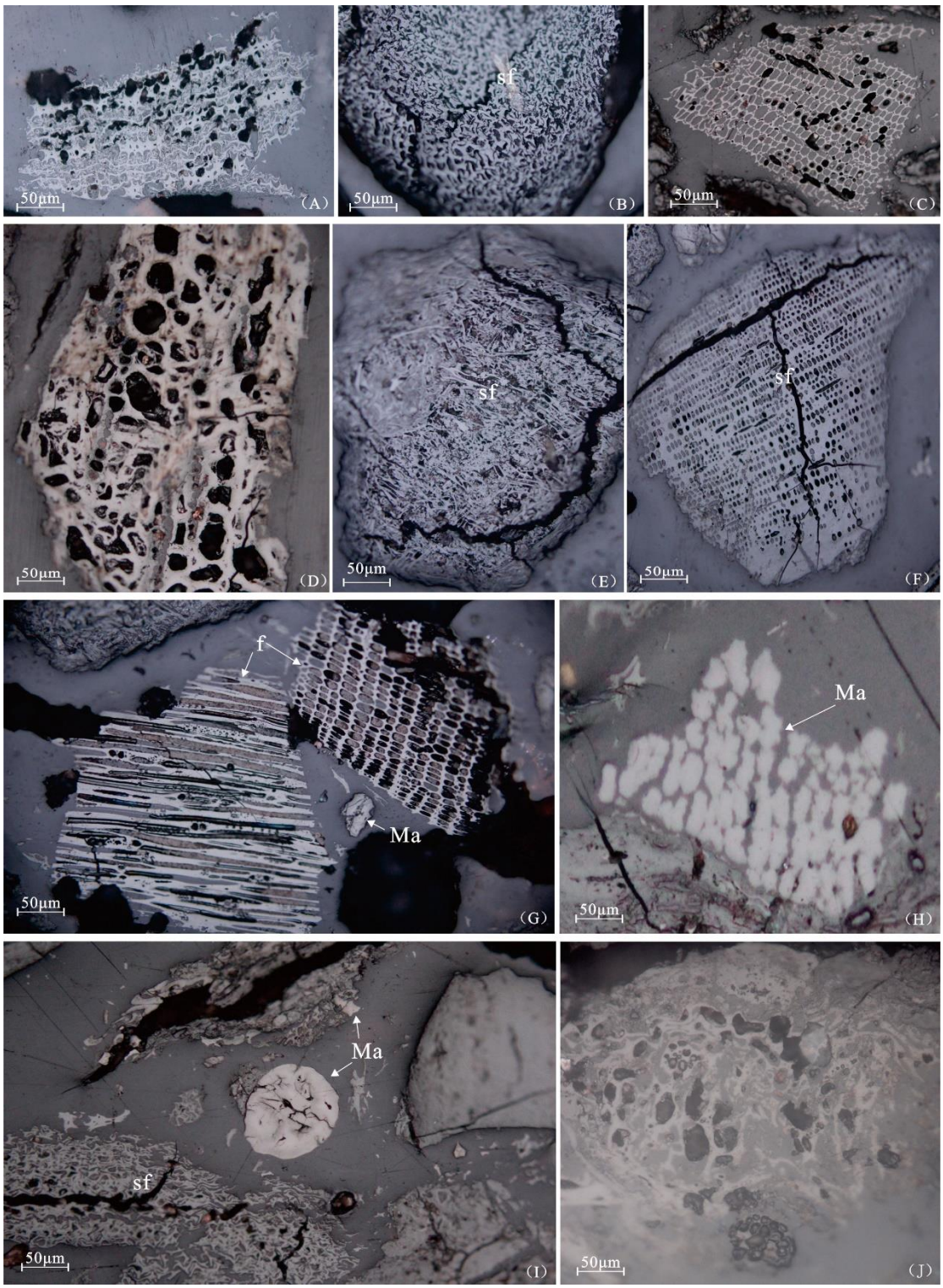
50μm
(A)
sf
50μm
(B)
50μm
(C)
50μm
(D)
sf
50μm
(E)
sf
50μm
(F)
f
Ma
50μm
(G)
Ma
50μm
(H)
Ma
sf
50μm
(I)
50μm
(J)

Figure 8

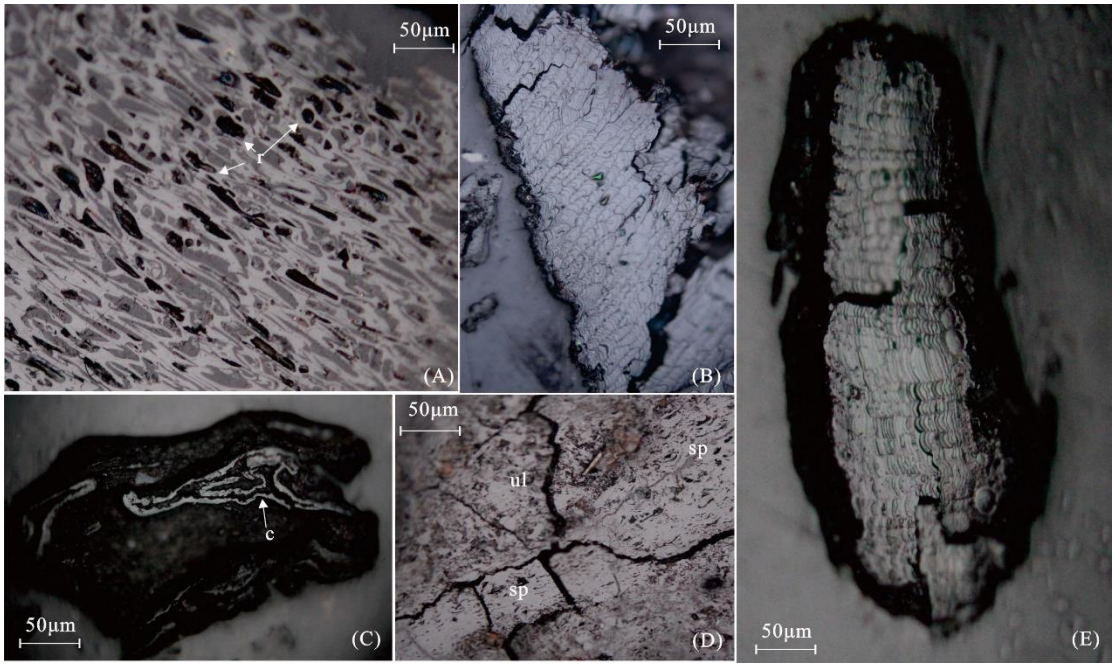

Figure 9

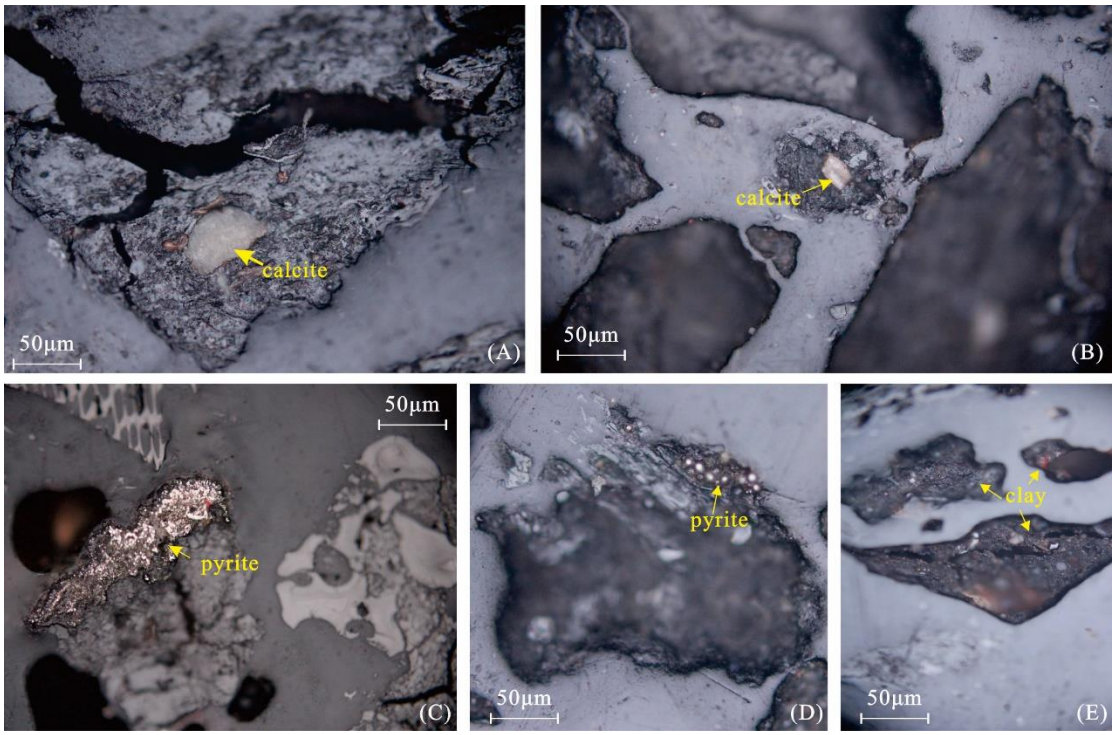
calcite
50μm
(A)
calcite
50μm
(B)
50μm
pyrite
(C)
pyrite
50μm
(D)
clay
50μm
(E)

1045 Figure 10

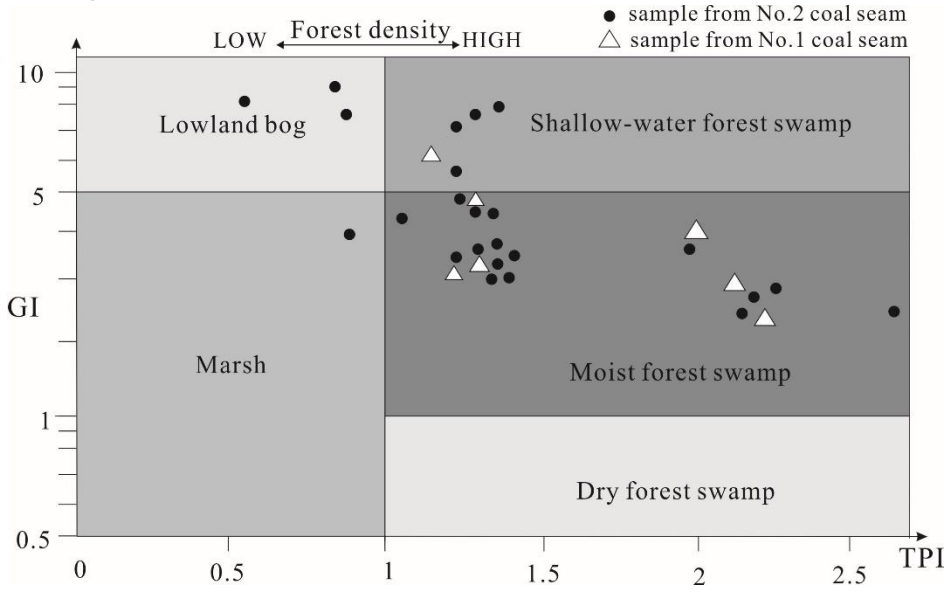

1046
1047

Figure 11

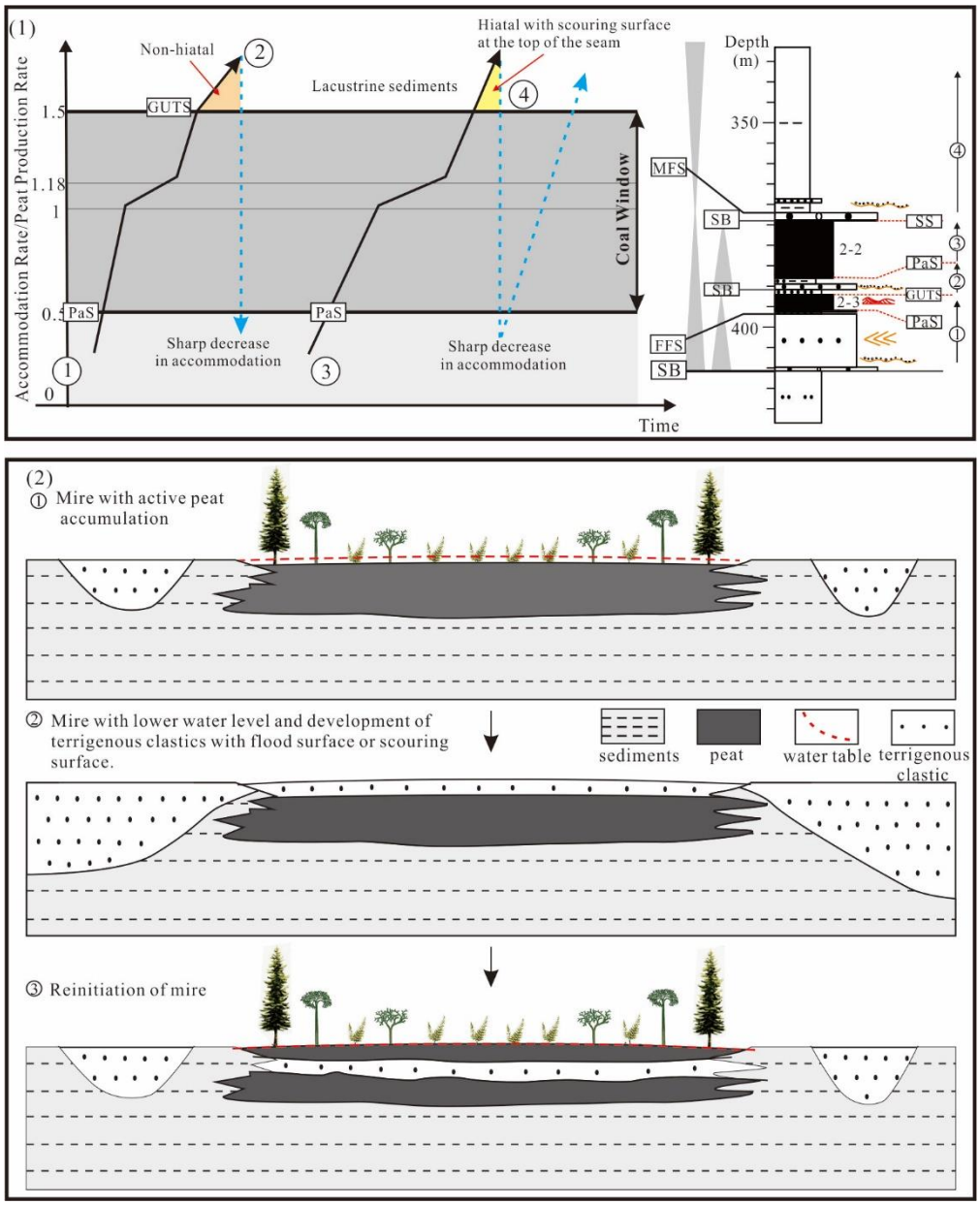
(1)
Non-hiatal
Hiatal with scouring surface at the top of the seam
Lacustrine sediments
GUTS
PaS
Sharp decrease in accommodation
Sharp decrease in accommodation
Coal Window
Accommodation Rate/Peat Production Rate
1.5
1.18
1
0.3
0
Time
Depth (m)
350
400
MFS
SB
SS
2-2
PaS
SB
GUTS
2-3
PaS
FFS
SB
(2)
① Mire with active peat accumulation
② Mire with lower water level and development of terrigenous clastics with flood surface or scouring surface.
sediments
peat
water table
terrigenous clastic
③ Reinitiation of mire

1052 Figure 12

1053

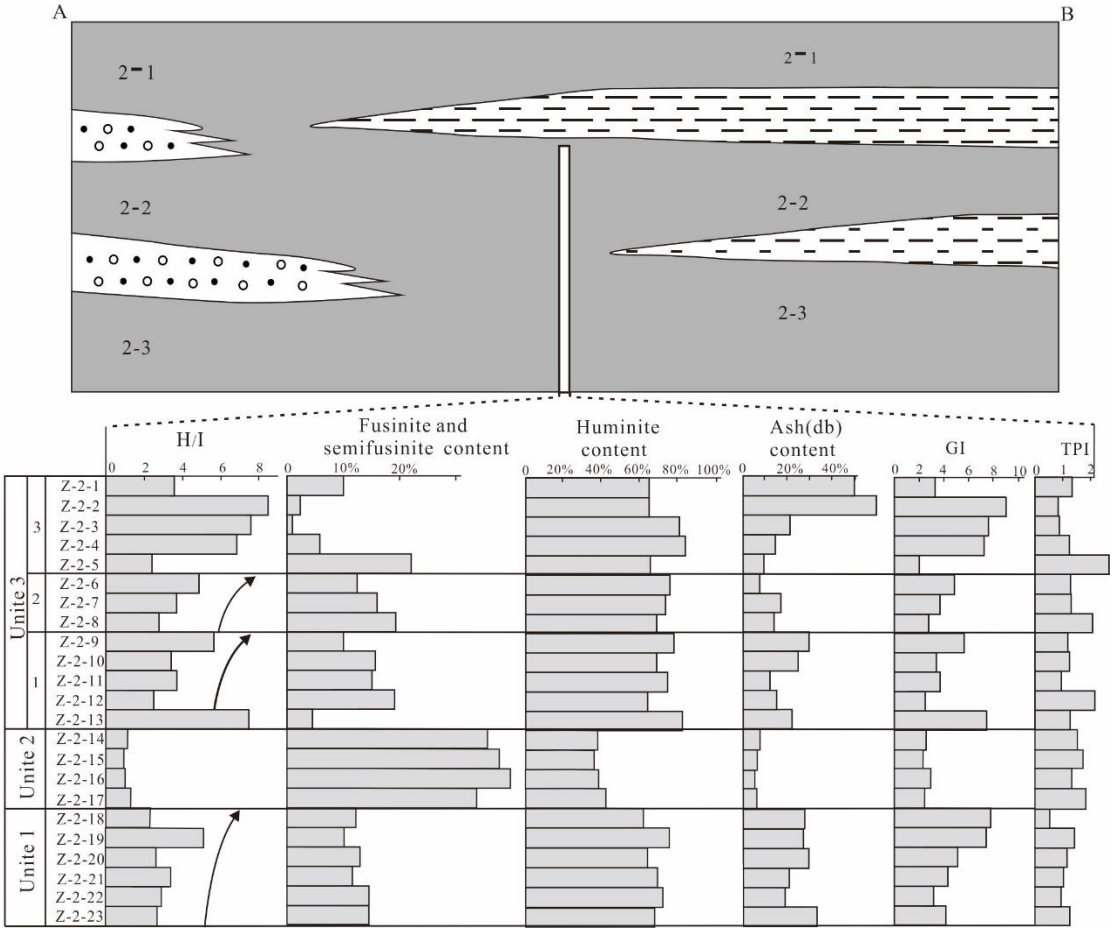

1054

1055

Figure 13

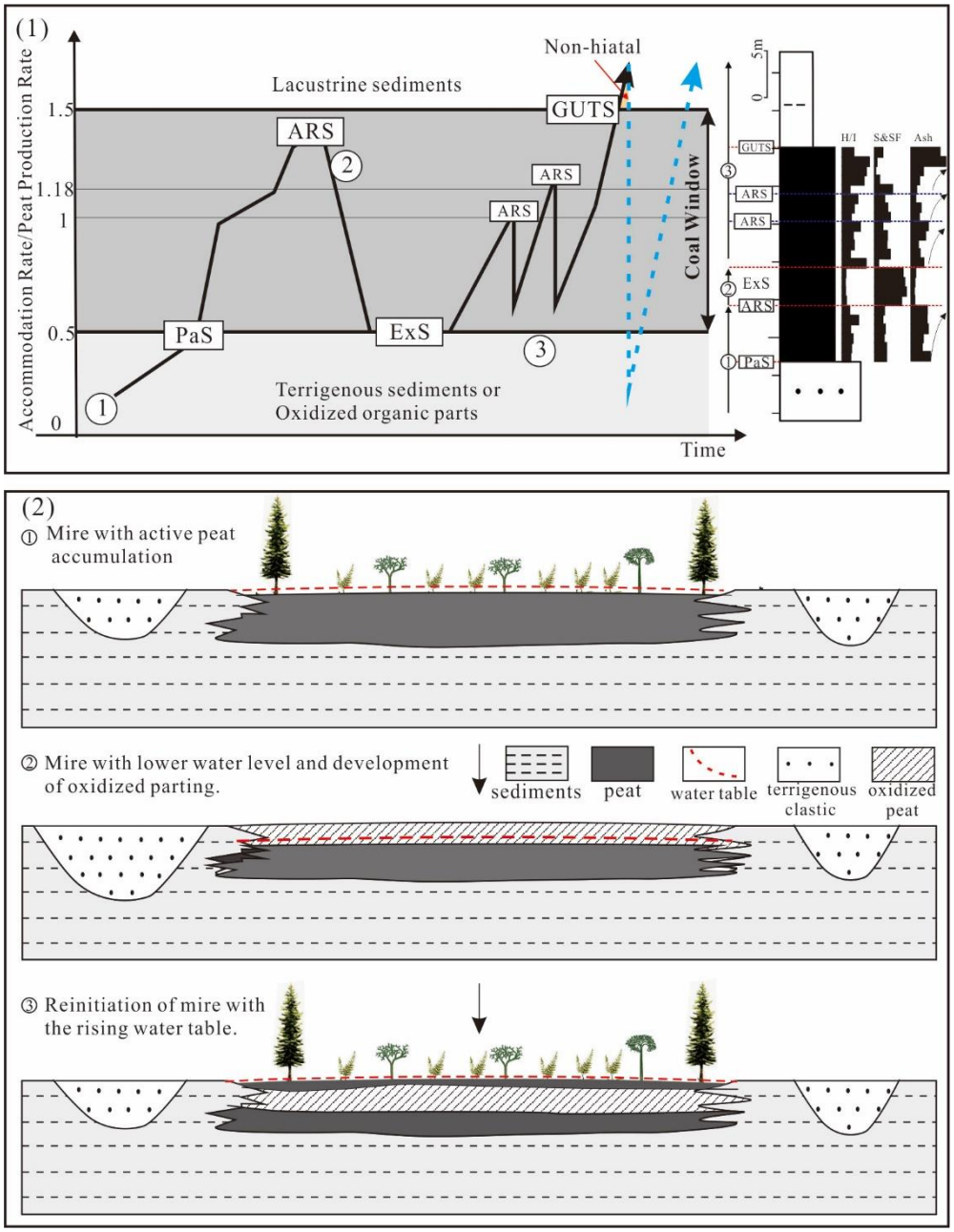
(1)
Accommodation Rate/Peat Production Rate
1.5
1.18
1
0.5
0
Lacustrine sediments
Non-hiatal
GUTS
ARS
ARS
ARS
PaS
ExS
Terrigenous sediments or
Oxidized organic parts
Coal Window
Time
5m
0
H/I
S&SF
Ash
GUTS
ARS
ARS
ExS
ARS
PaS
(2)
① Mire with active peat accumulation
② Mire with lower water level and development of oxidized parting.
sediments
peat
water table
terrigenous clastic
oxidized peat
③ Reinitiation of mire with the rising water table.

Figure 14

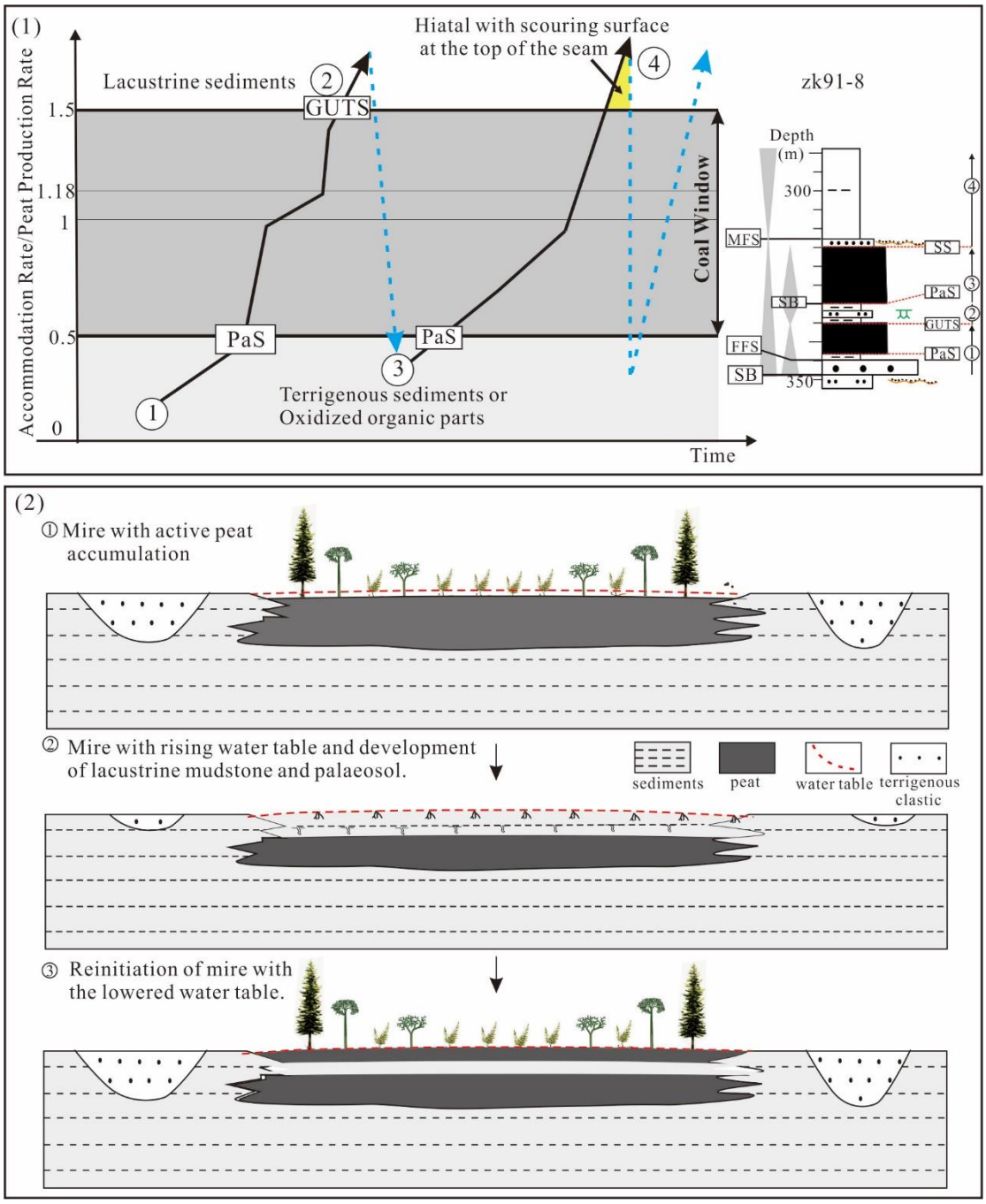
(1)
Accommodation Rate/Peat Production Rate
1.5
1.18
1
0.5
0
Lacustrine sediments
GUTS
PaS
PaS
Hiatal with scouring surface
at the top of the seam
Terrigenous sediments or
Oxidized organic parts
Coal Window
Time
zk91-8
Depth
(m)
300
350
MFS
SS
SB
PaS
GUTS
FFS
SB
PaS
(2)
① Mire with active peat
accumulation
② Mire with rising water table and development
of lacustrine mudstone and palaeosol.
sediments
peat
water table
terrigenous
clastic
③ Reinitiation of mire with
the lowered water table.

1064 Figure 15

1065

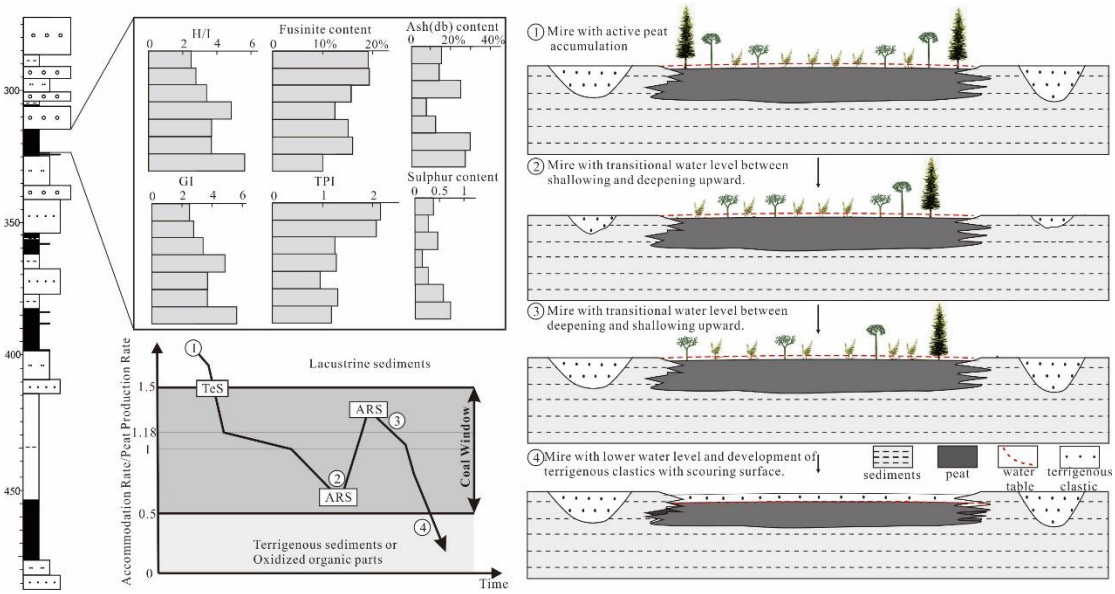

1066

1067

1068 Figure 16

1069

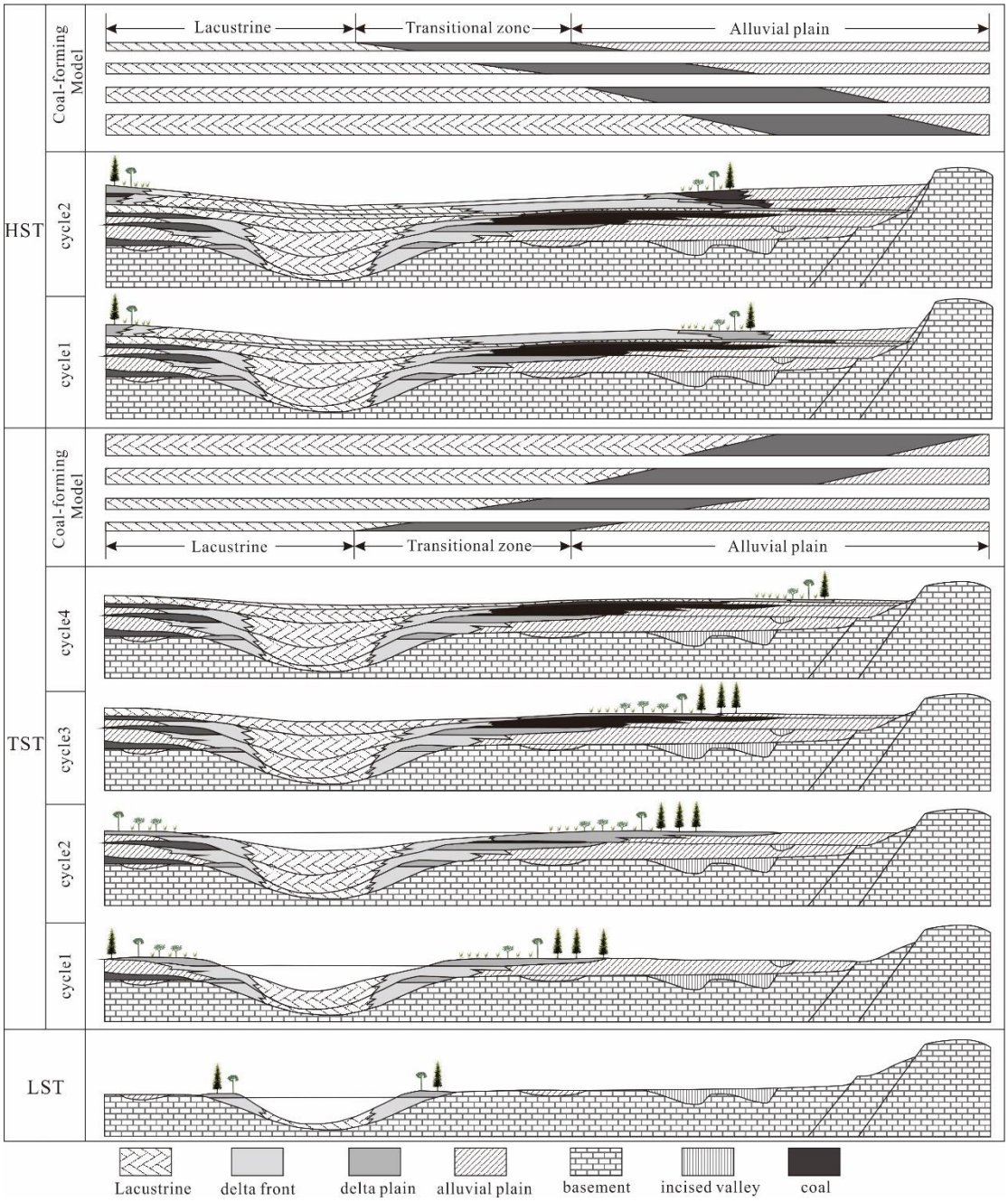

1070

1071

Figure 17

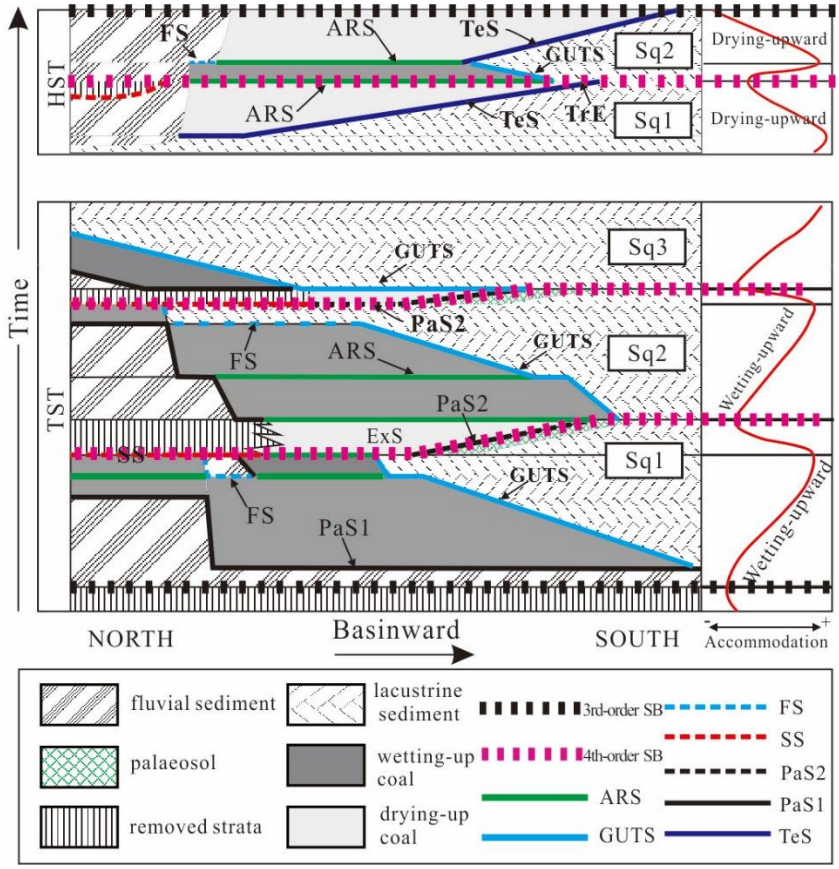
HST
TST
Time
FS
ARS
TeS
GUTS
Sq2
Drying-upward
TrE
Sq1
Sq3
PaS2
SS
ExS
PaS1
Wetting-upward
NORTH
Basinward
SOUTH
Accommodation
fluvial sediment
lacustrine sediment
palaeosol
wetting-up coal
removed strata
drying-up coal
3rd-order SB
4th-order SB

Table1

Yimin Formation	Sequence	Sag	DM	ZLNR	HHH	YM	HQ	WRX	HEHD	MDMJ	JQ	BR	MDH
	HST	late	—	▲	—	▲	—	—	▲	—	—	—	▲
		middle	▲	—	▲	—	▲	—	—	▲	▲	—	▲
		early	—	—	—	▲	—	—	—	—	—	▲	—
	TST	late	—	—	—	—	—	—	—	—	▲	—	—
		middle	▲	▲	▲	▲	—	▲	▲	—	—	—	—
		early	▲	▲	▲	▲	—	▲	▲	▲	▲	▲	▲
	LST	late	—	—	▲	—	—	—	—	—	—	—	—
		middle	—	—	—	—	—	—	—	—	—	—	—
		early	—	—	—	—	—	—	—	—	—	—	—

Table 2

Sample	M_{ad}/%	A_d/%	V_{daf}/%	$S_{t.d}$/%
Z-2-1	4.39	49.45	56.66	1.65
Z-2-2	8.69	55.42	52.88	1.75
Z-2-3	10.63	20.54	46.17	0.86
Z-2-4	10.15	14.03	46.40	0.36
Z-2-5	9.30	9.71	42.63	0.98
Z-2-6	9.07	8.20	44.73	0.15
Z-2-7	9.13	17.91	44.97	0.85
Z-2-8	9.78	13.53	44.77	0.26
Z-2-9	10.30	29.21	46.92	1.19
Z-2-10	8.97	24.78	46.62	0.88
Z-2-11	9.66	11.40	44.09	0.25
Z-2-12	10.78	14.54	43.91	0.32
Z-2-13	9.96	22.73	47.54	0.91
Z-2-14	8.83	7.92	43.93	0.22
Z-2-15	8.53	7.87	42.79	0.18
Z-2-16	9.01	7.69	41.90	0.20
Z-2-17	8.21	7.76	43.76	0.19
Z-2-18	8.73	23.91	46.09	0.89
Z-2-19	9.70	23.45	44.80	0.72
Z-2-20	10.02	28.18	46.69	0.84
Z-2-21	9.86	22.43	45.35	0.35
Z-2-22	9.63	20.49	45.35	0.50
Z-2-23	9.85	28.28	46.18	0.33

Table 3

Sample	T-I	T-H	F	HT	HD	HC	ID	H/I	Min
Z-2-1	17.33	63.22	10.04	39.36	13.58	10.27	7.29	3.65	17.87
Z-2-2	7.78	64.47	2.80	37.95	20.36	6.15	4.98	8.29	27.24
Z-2-3	10.94	82.10	1.52	36.35	29.48	16.27	9.42	7.51	6.90
Z-2-4	12.29	83.62	6.07	42.64	29.31	11.66	6.22	6.81	3.86
Z-2-5	27.56	64.50	24.09	40.73	11.75	12.02	3.47	2.34	6.12
Z-2-6	15.72	77.49	12.78	37.35	30.90	9.24	2.94	4.93	6.39
Z-2-7	19.90	73.97	16.13	38.65	34.57	0.75	3.77	3.72	5.50

Z-2-8	24.70	67.64	19.28	46.28	18.59	2.76	5.42	2.74	6.36
Z-2-9	13.96	80.09	9.67	44.10	35.11	0.87	4.29	5.74	5.76
Z-2-10	21.46	70.36	15.54	28.90	23.76	17.71	5.93	3.28	7.83
Z-2-11	19.91	72.17	14.98	48.34	19.88	3.94	4.93	3.63	6.42
Z-2-12	27.33	62.35	18.89	44.42	12.35	5.58	8.44	2.28	7.04
Z-2-13	11.39	83.18	5.62	43.59	27.54	12.05	5.78	7.30	5.25
Z-2-14	46.32	48.41	34.12	27.63	8.06	12.72	12.20	1.05	3.82
Z-2-15	48.53	47.37	37.07	26.47	9.32	11.37	11.21	0.98	3.23
Z-2-16	48.45	48.57	39.21	24.56	11.19	10.90	9.01	1.00	2.75
Z-2-17	42.64	53.21	30.91	26.73	10.42	14.89	10.53	1.25	3.07
Z-2-18	30.79	62.12	12.71	36.02	15.26	10.84	18.08	2.02	6.62
Z-2-19	15.19	77.51	10.04	37.56	36.04	3.91	5.15	5.10	6.11
Z-2-20	28.36	63.25	12.85	40.42	17.62	5.21	15.51	2.23	5.23
Z-2-21	22.82	70.10	11.56	44.23	24.25	1.62	11.26	3.07	5.01
Z-2-22	24.83	70.47	14.65	38.02	25.45	7.00	10.18	2.84	4.64
Z-2-23	25.56	68.25	14.63	42.24	22.23	13.78	10.93	2.67	4.94
Z-1-1	27.26	61.74	18.72	44.83	11.35	5.55	8.54	2.26	7.20
Z-1-2	24.64	66.98	19.11	46.71	17.51	2.75	5.53	2.72	6.51
Z-1-3	21.40	69.67	15.40	29.16	22.88	17.63	6.01	3.26	8.02
Z-1-4	15.68	76.73	12.67	37.69	29.83	9.20	3.01	4.89	6.54
Z-1-5	19.86	71.46	14.85	48.79	18.74	3.92	5.01	3.60	6.57
Z-1-6	19.85	73.24	15.99	39.01	33.49	0.75	3.86	3.69	5.63
Z-1-7	13.93	79.30	9.58	44.51	33.92	0.87	4.34	5.69	5.90